Natural Resources Canada
Ressources naturelles Canada

Geophysical logging methods for uranium geology and exploration

C.J. Mwenifumbo and A.L. Mwenifumbo

Geological Survey of Canada

Technical Note 4

2013

Canada

Geological Survey of Canada
Technical Note 4

Geophysical logging methods for uranium geology and exploration

C.J. Mwenifumbo and A.L. Mwenifumbo

2013

ISSN 1914-525X
Catalogue No. M41-10/4-2013E-PDF
ISBN 978-1-100-21750-5
doi:10.4095/292248

A copy of this publication is also available for reference in depository libraries across Canada through access to the Depository Services Program's Web site at http://dsp-psd.pwgsc.gc.ca

This publication is available for free download through GEOSCAN http://geoscan.ess.nrcan.gc.ca

Recommended citation
Mwenifumbo, C.J. and Mwenifumbo, A.L., 2013. Geophysical logging methods for uranium geology and exploration; Geological Survey of Canada, Technical Note 4, 43 p. doi:10.4095/292248

Critical review
C. Jefferson

Authors
C.J. Mwenifumbo (cjmwenifumbo@gmail.com)
A.L. Mwenifumbo (almwenifumbo@shaw.ca)
515 Fourth Street
New Westminster
British Columbia
V3L 2V7

Correction date:

Geophysical logging methods for uranium geology and exploration

C.J. Mwenifumbo and A.L. Mwenifumbo

Mwenifumbo, C.J. and Mwenifumbo, A.L., 2013. Geophysical logging methods for uranium geology and exploration; Geological Survey of Canada, Technical Note 4, 43 p. doi:10.4095/292248

Abstract: In the uranium mining industry, borehole logging is a basic tool in the exploration and delineation of uranium deposits. Whereras gamma-ray logging is recognized as one of the most effective techniques for delineating uranium mineralization and estimating uranium ore grade, there are several other methods that provide additional information on the stratigraphy, lithology, structures, and alteration associated with mineralization. These include resistivity, induced polarization, sonic P-wave velocity, density, and temperature.

This technical note provides a brief overview of uranium deposit types and describes at a very basic level the physical principles underlying various borehole-logging methods, equipment, data-acquisition procedures, and log interpretation. A few field case examples are presented. It also provides information on the calibration protocols for gamma-ray logging systems and calibration facilities that ensure reliable logging and interpretation are achieved.

Radioactivity occurs when particles and gamma rays are emitted as a nucleus spontaneously disintegrates. During radioactive decay, alpha particles, beta particles, and gamma rays are emitted. In uranium exploration the focus is on the gamma rays. Though there are three major naturally occurring uranium isotopes, ^{238}U, ^{235}U, and ^{234}U, 99.3% of natural uranium is ^{238}U. Therefore, assuming the parent product is ^{238}U, it decays by emitting beta particles, alpha particles, and gamma rays to its final state of lead-206 (^{206}Pb). The gamma rays that are detected in uranium exploration are from its daughter products, lead-214 (^{214}Pb) and bismuth-214 (^{214}Bi) and not from the parent ^{238}U.

Résumé : Dans l'industrie minière de l'uranium, la diagraphie en sondage est un outil de base pour l'exploration et la délimitation des gîtes d'uranium. Alors que la diagraphie de rayonnement gamma est reconnue comme étant l'une des techniques les plus efficaces pour délimiter la minéralisation uranifère et estimer la teneur en uranium du minerai, il existe plusieurs autres méthodes permettant d'obtenir de l'information supplémentaire concernant la stratigraphie, la lithologie, les structures et les altérations associées à la minéralisation. Ces méthodes ont recours entre autres à la résistivité, la polarisation provoquée, la vitesse des ondes longitudinales (P) acoustiques, la densité et la température.

La présente note technique offre un bref survol des types de gîtes d'uranium et fournit une description sommaire des principes physiques sur lesquels reposent différentes méthodes de diagraphie en sondage, de l'équipement, des procédures d'acquisition de données et de l'interprétation des données diagraphiques. On y présente quelques exemples d'études sur le terrain. On y fournit également de l'information sur les protocoles d'étalonnage des systèmes de diagraphie de rayonnement gamma et des installations d'étalonnage assurant la fiabilité des diagraphies et de leur interprétation.

La radioactivité correspond à l'émission de particules et de rayons gamma au moment de la désintégration spontanée d'un noyau. Pendant la désintégration radioactive, il y a émission de particules alpha, de particules bêta et de rayons gamma. Pour ce qui est de la prospection de l'uranium, ce sont les rayons gamma qui présentent le plus grand intérêt. Bien qu'il existe trois principaux isotopes naturels de l'uranium (^{238}U, ^{235}U et ^{234}U), 99,3 % de l'uranium naturel est de la forme ^{238}U. Aussi, en supposant que l'isotope père est le ^{238}U, l'uranium se désintègre en émettant des particules bêta, des particules alpha et des rayons gamma jusqu'à ce qu'il atteigne son état final de plomb 206 (^{206}Pb). Les rayons gamma qui sont détectés au cours de la prospection de l'uranium proviennent de ses produits de filiation, le plomb 214 (^{214}Pb) et le bismuth 214 (^{214}Bi), et non du ^{238}U père.

INTRODUCTION

The purpose of this technical note is to pass on to the mining community the benefit of borehole logging research at the Geological Survey of Canada (GSC), especially as applied to uranium exploration. It is based on material from the Uranium Logging Short Course that was presented by the GSC, Saskatchewan Research Council (SRC), and Saskatchewan Geological Survey (SGS) at the 2008 Saskatchewan Open House.

In recent years, intensive efforts in uranium exploration have stimulated research and development of new methods of borehole-logging analysis and interpretation. Borehole logging is one of the most effective ways of rapidly and economically measuring uranium in situ. It also plays an important part in providing consistent and reliable lithology and stratigraphic information. Physical rock-property, geotechnical, and groundwater-flow information can be extracted from the geophysical logging data and used in constraining the interpretation of other ground and airborne geophysical data.

The broad goals of this technical note are threefold: 1) to provide a brief overview of uranium deposit types; 2) to describe, at a very basic level, borehole methods and equipment, data acquisition procedures, log interpretation, and data protocols; and 3) to provide information on calibration protocols and facilities.

URANIUM DEPOSIT TYPES AND GEOLOGY

Uranium is a relatively common, dense, radioactive metal that occurs naturally in the Earth's crust (at about 3 ppm). A concentration of uranium in the environment (0.01–20%) is a 'uranium deposit'. The distribution of uranium ore occurs worldwide with sizable deposits and mines in Australia, Canada, the former Soviet republics, Africa, and U.S.A. (World Nuclear Association, 2011)(Table 1).

Knowledge of the type of uranium deposit is one of the factors that determine the geophysical methods that can be used during exploration, reserve delineation, and grade estimation. According to the International Atomic Energy Agency (IAEA), 15 types of uranium deposits have been identified based on the geology of the deposits (International Atomic Energy Agency, 2009).

These are unconformity-related, sandstone, quartz-pebble conglomerate, vein-type, breccia complex (IOCG-U), pegmatite-intrusive, phosphorite, collapse-breccia pipe, volcanic, surficial, metasomatite, metamorphic, lignite, black shale, and other types.

This note will focus on the top six deposit types, based on ore production. The same format will be followed for each type by describing a model of the deposit, the minerals associated, and examples of where the deposit type occurs.

Unconformity-related deposits

Proterozoic unconformity deposits are the world's main source of uranium, constituting more than 33%. These deposits are close to major unconformities that separate basement, commonly metamorphic rock, from overlying clastic sedimentary rocks. The orebodies are pod, lens, or vein in shape and often occur along fractures and/or fault zones (Fig. 1). Typical minerals found in these deposits are uraninite (also known as pitchblende) and coffinite with variable nickel, cobalt, lead, arsenic, and traces of gold, platinum, rare-earth elements, and iron (Jefferson et al., 2007).

Major sites for unconformity-related deposits are Canada (Athabasca Basin, Saskatchewan and Thelon Basin, Northwest Territories); and Australia (the Alligator Rivers region, Northern Territory and Rudall River area, Western Australia) (World Nuclear Association, 2010).

Sandstone deposits

Sandstone uranium deposits make up about 18% of the world's resources. The grades in sandstone deposits are low to medium (0.05–0.5% U_3O_8). The main uranium minerals are uraninite and coffinite. There are three main types of sandstone deposits: roll front, tabular, and tectonic and/or lithological (World Nuclear Association, 2010).

The roll-front model in Figure 2 shows that the sandstone units containing the ore are confined by impermeable sedimentary rocks generally consisting of mudstone. Sandstone-type

Table 1. World uranium resources by country (International Atomic Energy Agency, 2009).

Country	Percentage
Australia	22.7%
Kazakhstan	14.9%
Russian Federation	10%
Canada	8.2%
South Africa	8.0%
USA	6.2%
Brazil	5.1%
Niger	5.0%
Namibia	3.8%
Uzbekistan	2.0%
India	1.3%
China	1.2%
Others	11.5%
Total	100.0%

deposits are found in the United States, Kazakhstan, Uzbekistan, Gabon, France, Niger, Russia, South Africa, and Australia (International Atomic Energy Agency, 2009).

Quartz-pebble conglomerate deposits

Quartz-pebble conglomerate uranium deposits make up about 13% of the world's uranium resources. The ore grades range from 0.01–0.15% U_3O_8. These types of deposits are found in Canada and South Africa (International Atomic Energy Agency, 2009).

Figure 3 shows a schematic of the deposit from Agnew Lake in the Blind River–Elliot Lake region in Canada. Note that the ore is in the thin red lines that are labelled 'uraniferous conglomerate'. A high degree of fracturing is also depicted in the model. In this area, the ore minerals include uraninite, coffinite, uranothorite, and brannerite. At the present time there is no active mining in the Elliot Lake area.

Vein-type deposits

In vein-type deposits, the uranium minerals fill veins, pore spaces, joints, and breccia units or stockworks, etc. Since there is so much variability in this type of deposit, it is not possible to give estimates of uranium concentrations or grades. The main minerals in these deposits are pitchblende (uraninite) and coffinite. Vein-type deposits are found in France and the Czech Republic (International Atomic Energy Agency, 2009).

Breccia-complex (IOCG-U) deposits

There is a major breccia-complex uranium deposit in Australia's famous Olympic Dam area. At this mine, uranium is a by-product of the mining of iron ore, copper, and gold. (That is where the acronym IOCG-U comes from.) The alteration type associated with this type of deposit is potassic. The grades are typically about 0.08% for breccia-complex deposits. Breccia-complex deposits are also found in South America and Canada (International Atomic Energy Agency, 2009).

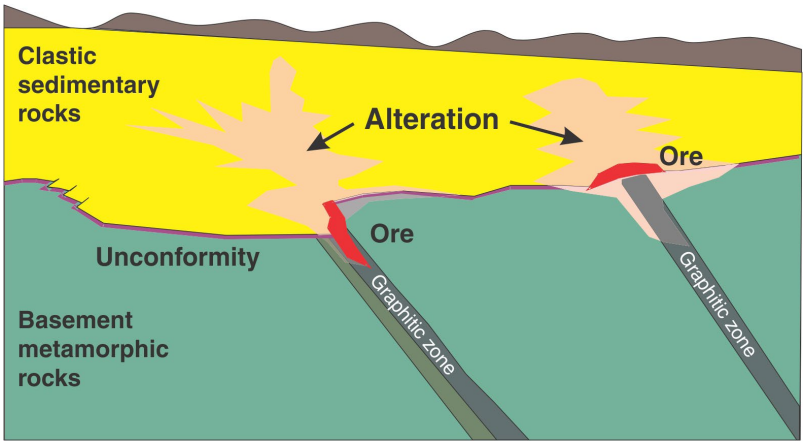

Figure 1. Model of an unconformity-related deposit (*modified from* Jefferson et al., 2007, Fig. 11) showing basement and unconformity deposits.

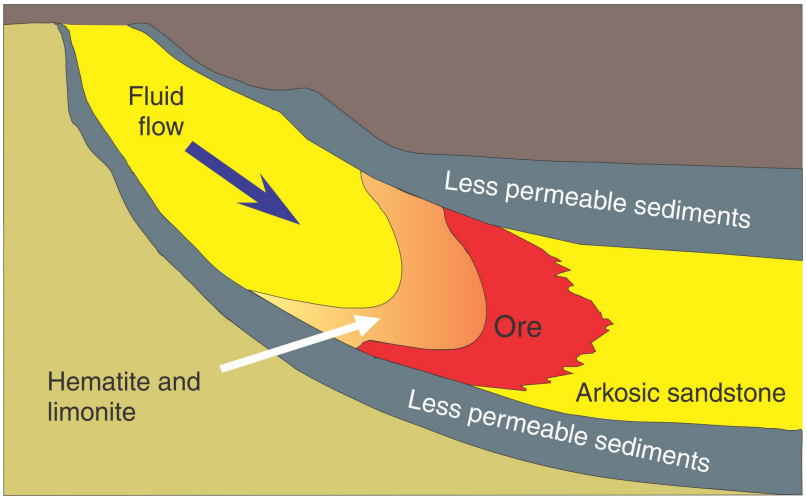

Figure 2. Model of a roll-front deposit (*modified from* Devoto, 1978).

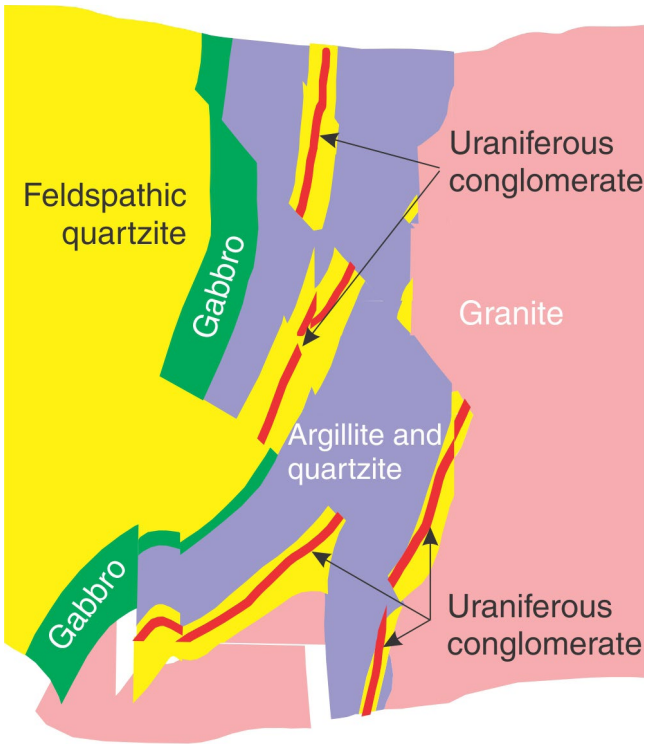

Figure 3. Model of a quartz-pebble conglomerate deposit (*modified from* McBride and Workman, 2005, Fig. 4).

Pegmatite-intrusive deposit

The last uranium deposit type is the pegmatite-intrusive type. The ore minerals associated with it vary, depending on the location of the deposit. In the Bancroft area in Ontario, the associated minerals are uraninite and other uranium-thorium minerals. At the Rossing deposit in Namibia, Africa, the uraninite is associated with copper-sulphide minerals, molybdenite, and iron-oxide minerals. These types of deposits are also found in Greenland, South Africa, and Australia (International Atomic Energy Agency, 2009).

The producers

Kazakhstan produces 33% of the world supply from mines, followed by Canada (18%), and Australia (11%) (World Nuclear Association, 2011). World uranium resources are listed in Table 1.

AN OVERVIEW OF LOGGING METHODS

There are several logging methods that are used in a variety of applications including mineral exploration, oil and gas exploration, and environmental and geotechnical problems. These methods include nuclear, electrical, magnetic, sonic, borehole imagery, and temperature and will be discussed in more detail in the sections to follow. In mineral exploration including uranium, logging is generally used to map lithology and correlate stratigraphy from drillhole to drillhole, to identify and map alteration associated with ore mineralization, to delineate ore mineralization, and to estimate ore grade in situ. Logging may also be used to provide information on groundwater flow patterns in joints and fractures intersected by the holes and to determine in situ physical-rock properties for use in interpreting data from other geophysical methods such ground and airborne.

This section covers the basic parts of logging systems, types of measurements that are of interest in uranium exploration, and how the borehole environment affects the choice of logging methods.

Logging-system components

The primary components of a logging system (Fig. 4) consist of a probe with geophysical sensor, a logging cable and winch for sending signals to surface instruments and electrical power down to the probe, a depth counter attached to a wellhead pulley for keeping track of the location of the probe in the hole, and uphole electronics connected to a laptop computer to aid in monitoring, analysis, and display of the data during acquisition.

Some systems are portable (Fig. 5) and others require a customized truck (Fig. 6). The choice used depends on the terrain, whether climate control is needed for the system, or if a large winch is necessary for a deep hole. Portable systems are particularly good in mining or when it is necessary to fly into a site.

Types of probes

Probes generally fall into two classes: passive and active. There are also other probes that are mainly used to investigate the borehole-wall characteristics and its trajectory.

Passive probes

In passive probes there is a single sensor or receiver that detects naturally occurring fields or physical processes (Fig. 7). The main formation parameters these types of probes measure are natural gamma-ray activity, self potential (sometimes known as spontaneous polarization potential), formation temperatures, and magnetic susceptibility. Passive probes also include those that provide information on fluid properties in the borehole such as temperature, flow, and fluid chemistry like Eh (REDOX potential) and pH. These types of measurements are useful in hydrogeological and/or hydrogeochemical investigations.

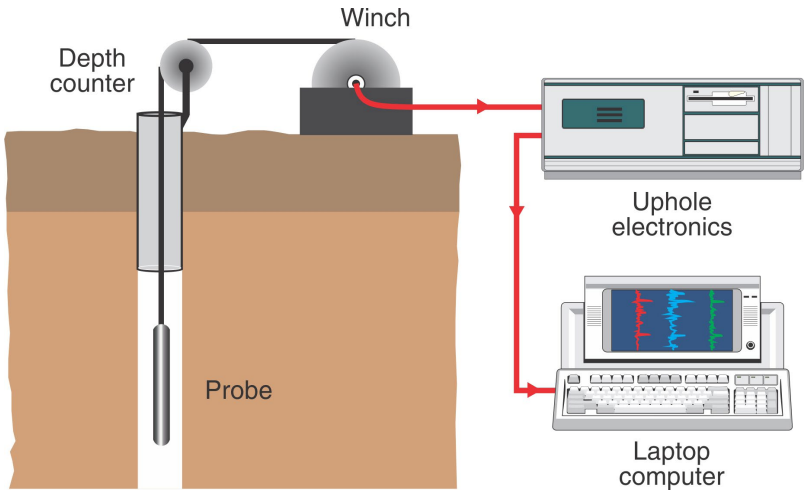

Figure 4. Logging-system components.

Figure 5. Images of portable logging system in field operations; **a)** multiparameter probe and a winch out of the truck near the borehole; **b)** well-head pulley assembly with a portable winch and the data-acquisition system in the van, and **c)** GSC portable logging–data acquisition system, winch, and probe being used underground. Photographs by J. Mwenifumbo.

Active probes

There are several probes that can be grouped into the active category (Fig. 8a). Essentially these probes have a source or transmitter that generates an artificial field and these fields are detected by sensor, receiver, or detector. Some of these probes are:

1. Density probe: has a gamma-ray (radioactive) source and a gamma-ray detector;
2. Resistivity probe: has a transmitter that is used to inject a current into the formation and the potential field created is measured with a voltmeter;
3. Induced-polarization (IP) probe: works in the same manner as the resistivity probe in that there is a current transmitter and a potential measuring device;
4. Sonic probe: has a transmitter that generates acoustic energy or seismic waves that are detected by a receiver such as a geophone, hydrophone, or seismometer;

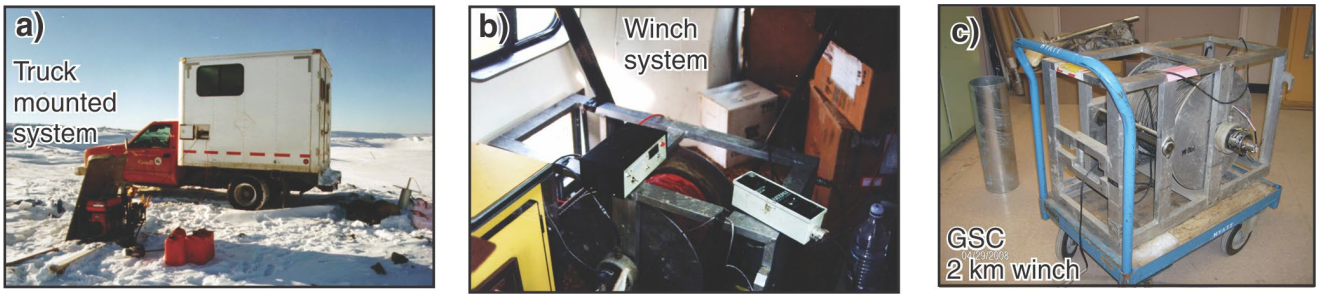

Figure 6. Geological Survey of Canada truck-mounted logging; **a)** logging truck, **b)** 2 km logging winch mounted in the truck, and **c)** 2 km logging system. Photographs by J. Mwenifumbo.

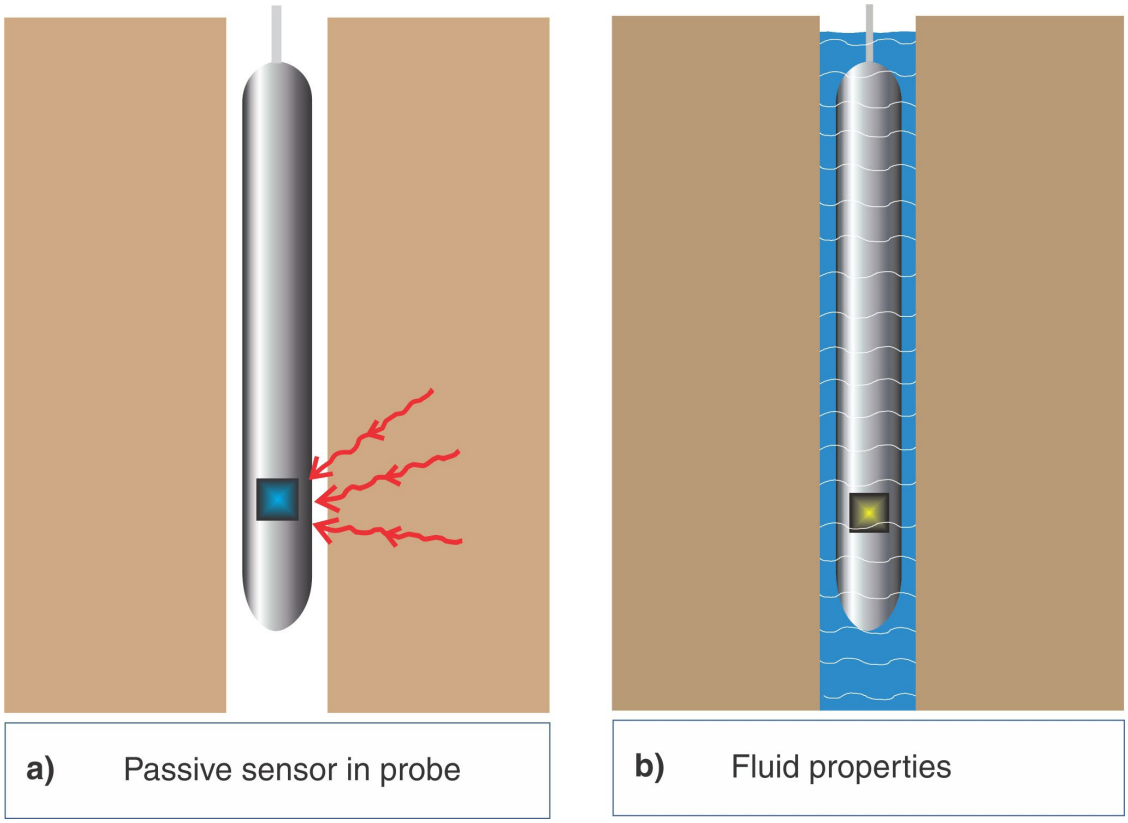

Figure 7. Passive probes used to measure **a)** formation parameters, and **b)** fluid properties.

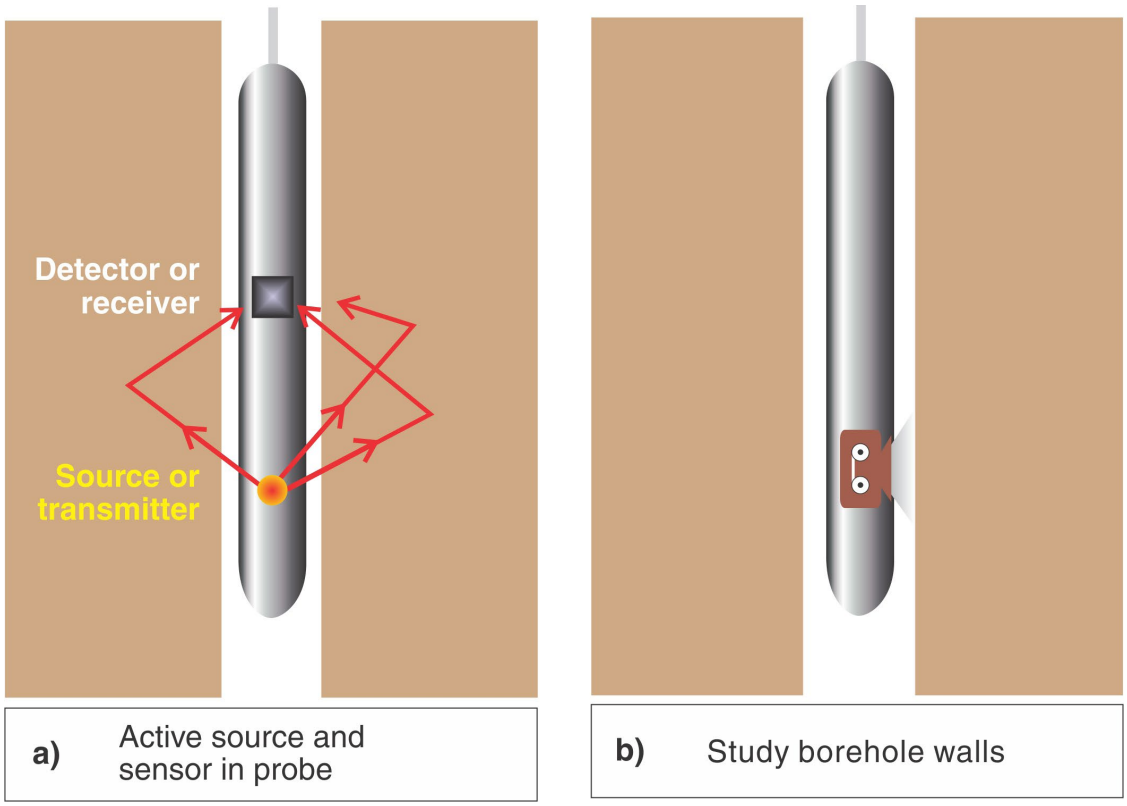

Figure 8. Probes with active sources and sensors **a)** for studying formation parameters, and **b)** for borehole-wall imaging.

5. Neutron porosity and prompt fission neutron probes: have a neutron source or neutron generator and neutron detector; and
6. X-ray fluorescence or XRF probe: has a gamma-ray source that illuminates the target with an intense X-ray beam. The excited sample in turn emits X-rays along a spectrum of wavelengths characteristic of the types of atoms present in the sample. These are picked up by a detector or receiver in the probe.

Borehole imaging

Borehole-imaging techniques can also be grouped into passive or active probes. The caliper probe is an example of a passive probe that measures the diameter of the hole. This measurement is used as a correction factor during well-log analysis.

The optical, acoustic, and electrical televiewers can be classed as active probes (Fig. 8b). The optical televiewer allows one to get optical views of the wall and is useful in locating structures such as faults and also bed boundaries where there is a significant change in rock-formation colours. Acoustic televiewer tools have a transmitter that scans the borehole wall with an acoustic beam and the acoustic energy reflected at the borehole fluid and rock interface is recorded by a receiver. The data are processed to an image of the surrounding formation. An electrical televiewer scans the borehole wall with small electrode arrays consisting of current electrodes (transmitters) and potential electrodes (receivers).

Knowing where a borehole goes in 3-D space is very important (Killeen et al., 1995). Figure 9 shows the various paths a borehole can take during drilling. There are a number of ways to survey a borehole and some of these include the standard Tropari, a compass, magnetometers, inclinometers, and gyros.

Types of borehole measurement configurations

In borehole logging, there are generally three types of measurements: single hole, surface-to-hole, and hole-to-hole or crossborehole. In single-hole measurement mode, all the transmitting and sensing or receiving of the signal is done in one hole. The probe contains both a receiver and a transmitter. Surface-to-hole measurements include pulse EM, directional induced polarization and resistivity, and vertical seismic profiling. In this case, a 'source' is located on the surface and the sensor is contained in the probe (Fig. 10).

Crossborehole or hole-to-hole methods include seismic, electrical, and radar (Fig. 11). In this methodology, at least two holes are used with a source or sources placed in

one hole while measurements are taken in the other hole. The transmitter may consist of current electrodes or acoustic transducers, for crossborehole electrical and seismic tomography, with corresponding potential electrodes or hydrophones, respectively.

Borehole environments

In addition to the exploration target, the borehole environment determines the type of measurements that can be made. The factors that describe the environment include hole size, presence or absence of casing (plastic or steel), and whether the hole is air- or water-filled (Fig. 12). Most modern 'slim-hole' probes (tools), 38–50 mm in diameter, are designed to run in BQ or larger holes. The logging speed is usually about 6 m/min. Data sampling rates range from 1 sample/s to 5 samples/s, and provide measurements every 2–10 cm along the hole. The importance of these borehole environmental factors will be further highlighted in later sections of this report.

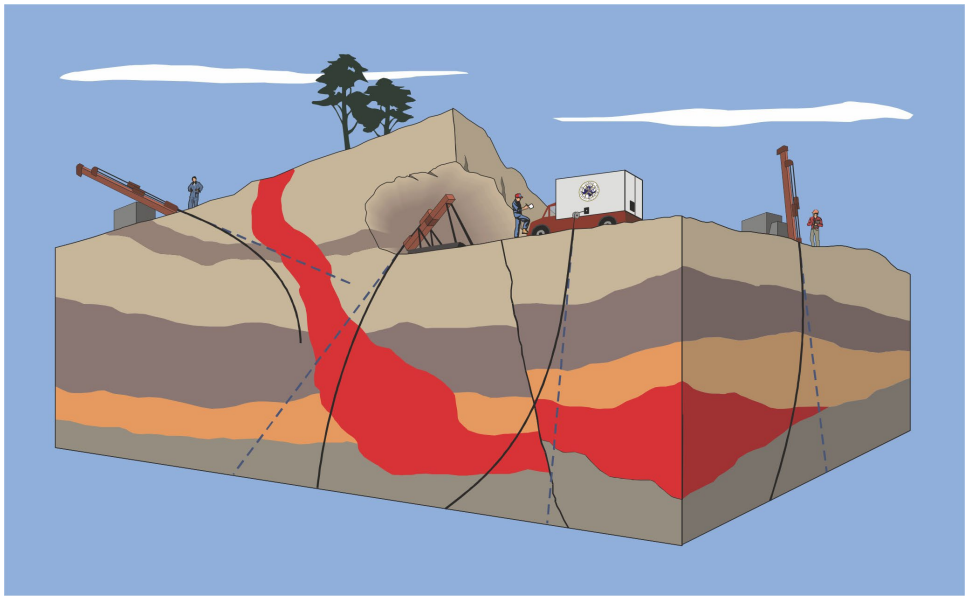

Figure 9. Surveying the path of the borehole with borehole orientation probes (*from* Killeen et al., 1995).

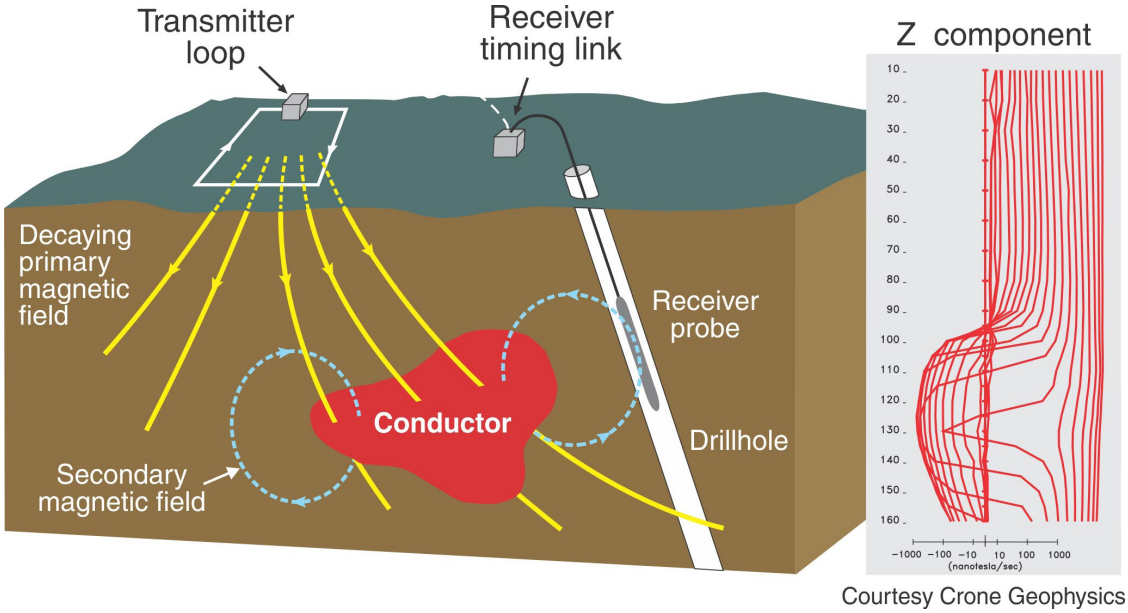

Courtesy Crone Geophysics

Figure 10. Surface-to-hole pulse EM layout (courtesy Crone Geophysics).

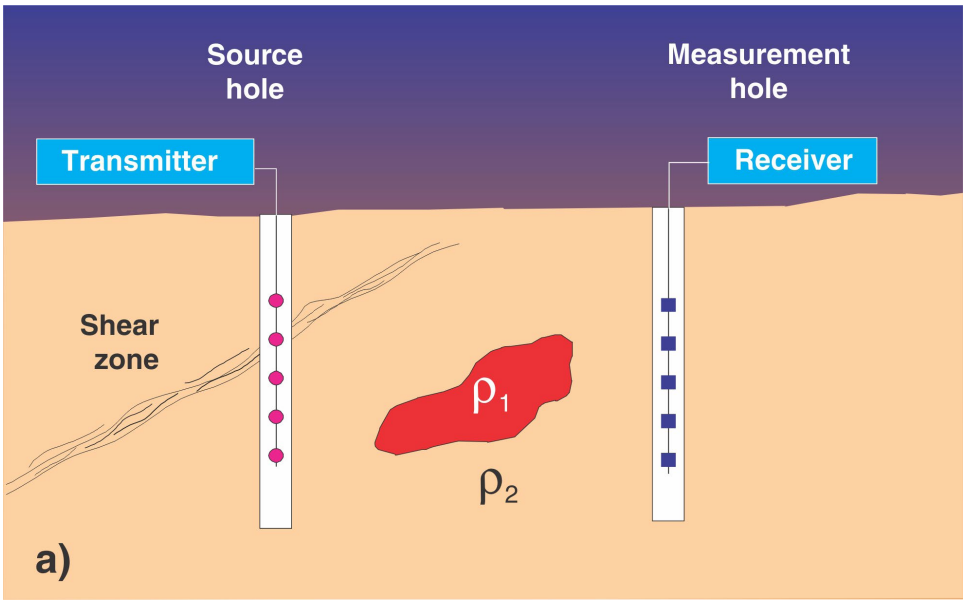

Figure 11. Configuration of cross-borehole or hole-to-hole method of measurements.

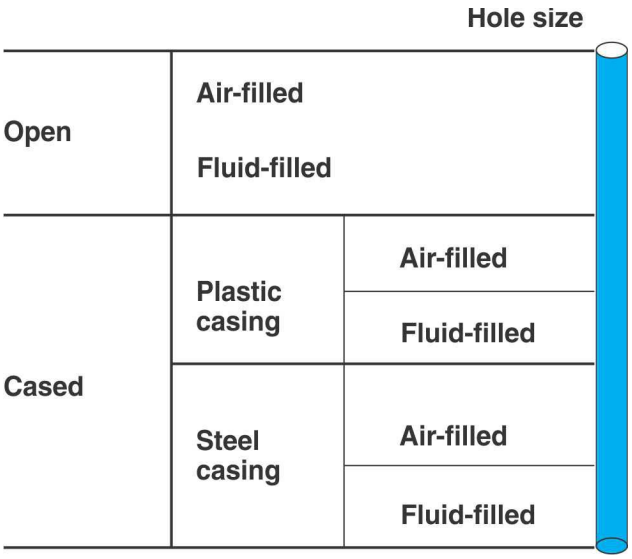

Figure 12. Different types of borehole environments that need to be considered when planning for logging.

GAMMA-RAY AND SPECTRAL GAMMA-RAY LOGGING

Introduction

Gamma-ray logging is the main borehole geophysical technique of interest in the exploration for uranium (Killeen, 1983). Gamma-ray measurements detect variations in the natural radioactivity originating from changes in concentrations of the trace elements uranium (U) and thorium (Th) as well as changes in the concentrations of the major rock-forming element, potassium (K). Since the concentrations of these naturally occurring radioelements vary between rock types, natural gamma-ray logging provides an important tool for mapping lithology and correlating stratigraphy. Gamma-ray logs are also important for detecting alteration zones, and for providing information on rock types. For example, in sedimentary rocks, sandstone can be easily distinguished from shale due to the low potassium content of the sandstone compared to the shale. In igneous and metamorphic geological environments, the three sources of natural radiation contribute equally to the total gamma-ray radiation detected by the gamma-ray probe. Often in base-metal and gold exploration areas, the principal source of the natural gamma-ray radiation is potassium because alteration, characterized by the development of sericite, is prevalent in some of the rock units and results in an increase in potassium. During metamorphism and hydrothermal alteration processes, uranium and thorium may be preferentially concentrated in certain rock units.

The radioelement concentrations of some common rocks in nature are shown in Table 2.

A gamma-ray probe's sensor is usually a sodium iodide or caesium iodide scintillation detector. Unlike a total-(gross) count gamma-ray probe, the spectral gamma-ray probe measures the energy of each gamma ray detected. Potassium, uranium, and thorium emit gamma rays with characteristic energies so estimates of the concentrations of the three radioelements can be made. Because there should be an equilibrium relationship between the daughter product and parent, it is possible to compute the quantity (concentration) of parent uranium (^{238}U) and thorium (^{232}Th) in the decay series by counting gamma rays from the daughter products ^{214}Bi and ^{208}Tl, respectively, if the probe has been properly calibrated.

Table 2. Radioelement concentrations of some major rock types (Killeen, 1979).

Rock class	K (%)	U (ppm)	Th (ppm)
Felsic (acid intrusive rocks)	0.10–7.6	0.10–30	0.10–253
Mafic (basic intrusive rocks)	0.02–2.6	0.01–5.7	0.03–15
Ultramafic and ultrabasic	0.00–0.8	0.00–1.6	0.00–7.5
Detrital sedimentary rocks	0.01–9.7	0.10–80	0.20–362
Metamorphosed igneous rocks	0.10–6.1	0.10–148.5	0.10–100

Basic terminology

Some basic terminology that is necessary to understand the principles of gamma-ray logging, is presented in Figure 13. These terms are all familiar, but the one to focus on is the 'Z'. Z-effects or Z-corrections will be discussed in 'How do gamma rays interact with matter?', but this is where the 'Z' comes from (as opposed to Z in statistical terminology).

Radioactivity occurs when particles and gamma rays are emitted as a nucleus spontaneously disintegrates. During radioactive decay, alpha particles, beta particles, and gamma rays are emitted. In uranium exploration the focus is on the gamma rays. Figure 14 shows what happens when uranium decays. Though there are three major natural-occurring uranium isotopes, ^{238}U, ^{235}U, and ^{234}U, 99.3% of natural uranium is ^{238}U. Therefore, assuming the parent product is ^{238}U, it decays by emitting beta particles, alpha particles, and gamma rays to its final state of lead-206 (^{206}Pb). The gamma rays that are detected in uranium exploration are from its daughter products, lead-214 (^{214}Pb) and bismuth-214 (^{214}Bi) and not from the parent ^{238}U.

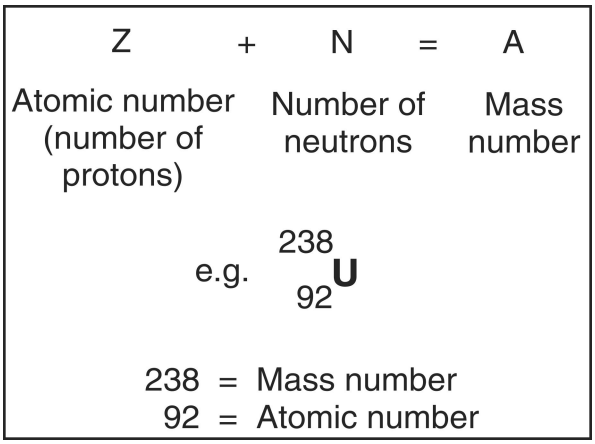

Figure 13. Elements are identified by their unique atomic numbers, Z. Uranium, for instance, has 92 protons (Z) and up to 146 neutrons (N) in the nucleus. The different isotopes are distinguished by their mass number; e.g. the three major natural-occurring uranium isotopes, ^{238}U, ^{235}U, and ^{234}U, have 146, 143, and 142, neutrons, respectively.

How do gamma rays interact with matter?

There are three main ways in which gamma rays interact with matter: photoelectric effect, Compton scattering, and pair production (Fig. 15). The photoelectric effect occurs when the gamma rays hit a material, are absorbed, temporarily raise the electron level in the material, and then decay. This occurs at low energies (less than 50 keV). In the case where the elements that make up the material have high atomic number (Z), you get what is known as the Z-effect (Dodd and Eschliman, 1972; International Atomic Energy Agency, 1986). No gamma rays reach the detector as they are absorbed by the material. Compton scattering occurs when gamma rays bounce back and forth from electron to electron, lose a little energy, and then reach the detector. This occurs at medium energies (100 keV to 10 MeV) and is the dominant process by which gamma rays interact with matter. Pair production occurs when the high-energy gamma rays interact with the nucleus of the material to produce a positron pair.

How are gamma rays detected?

There are two basic types of detectors commonly used in the uranium logging industry: scintillation and Geiger Müller. There are, however, several types of scintillation detectors. Three common ones are: 1) caesium iodide, sodium-doped (CsI(Na)); 2) sodium iodide, thallium-doped (NaI(Tl)); and 3) bismuth germinate (BGO), which is a very high-density material. The high-efficiency and large-volume detectors are preferred in low-grade U mineralization. They provide spectral coverage from about 0.1 MeV to 30 MeV. If used in high-grade uranium mineralization, they should be shielded. The Geiger Müller detectors are low efficiency and are preferred when evaluating high-grade uranium mineralization. Figure 16 shows a basic scintillation type of gamma-ray detector.

There are two types of logging systems used to measure gamma rays in a borehole. The first is the total- or gross-count logging system (Fig. 17), which is commonly used in the uranium exploration industry; however, it has no radioelement discrimination capability, so all the natural gamma rays from any radioactive sources are detected and appear in the log. The setting of the low-level discriminator (LLD) is critical in the total-count logging system. The LLD is the value for the low energy of the counting window. Lowering this value can cause false readings caused by noise. Raising this value can cause some of the lower energy sources to be missed.

The second system is gamma-ray spectrometry (Fig. 18). This is generally set as a four-window system: the total-count, potassium, uranium, and thorium windows. Presently, there are several systems that measure a complete energy spectrum from approximately 0.1 MeV to 3.0 MeV. The gamma rays are counted in several channels usually at 12 keV per

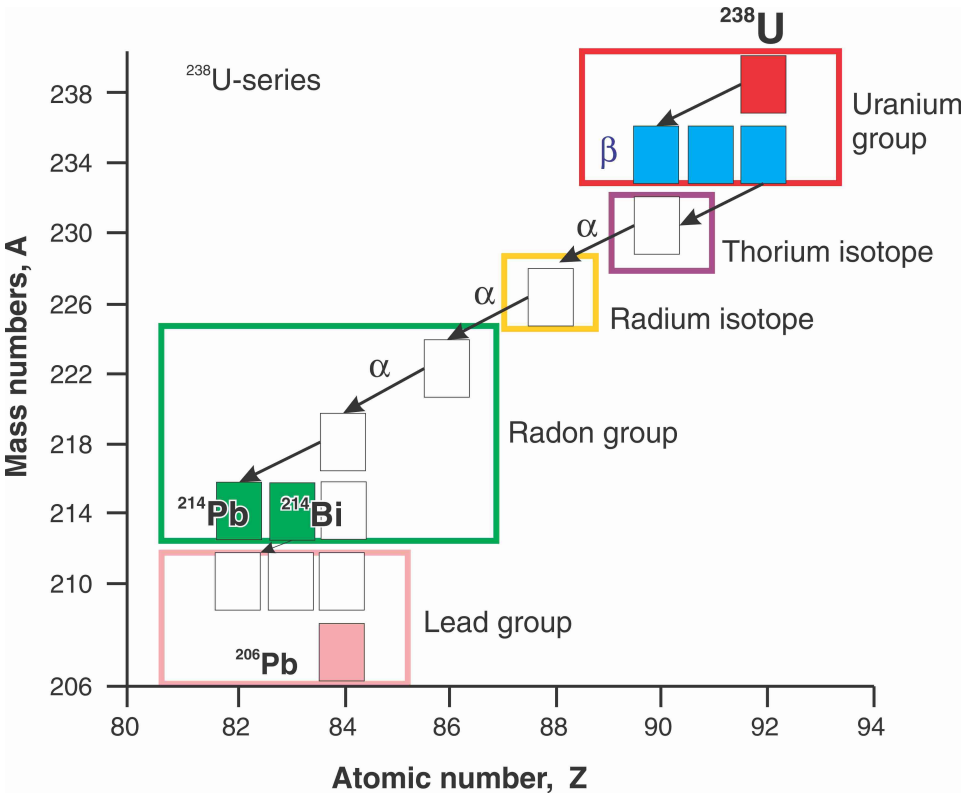

Figure 14. Uranium-238 decay series showing the five major equilibrium groups and radiation emitted during the decay process (*modified from* Killeen 1983). The gamma radiation that is monitored comes from the decay of ^{214}Pb and ^{214}Bi. The final end product is the nonradioactive ^{206}Pb.

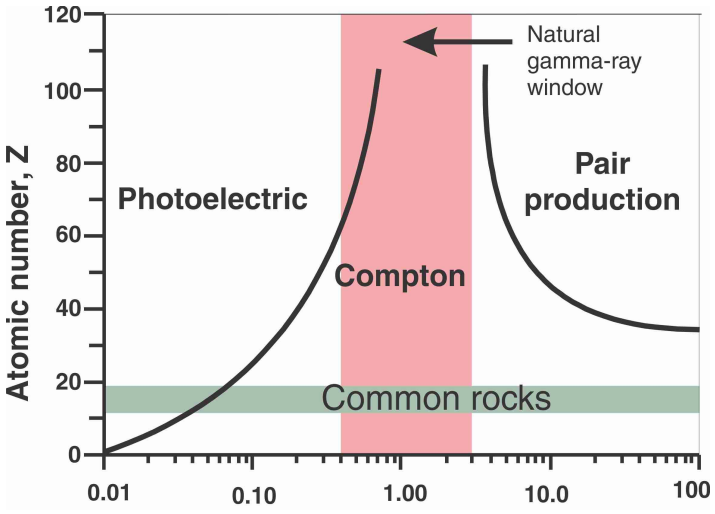

Figure 15. Gamma-ray interaction with matter (*modified from* Dodd and Eschliman, 1972). The pink highlighted area shows the standard GSC total-count measurement energy window (0.4–3.0 MeV). In this energy window the interaction of gamma rays with common rocks (Z between 10 and 20) is primarily by Compton scattering.

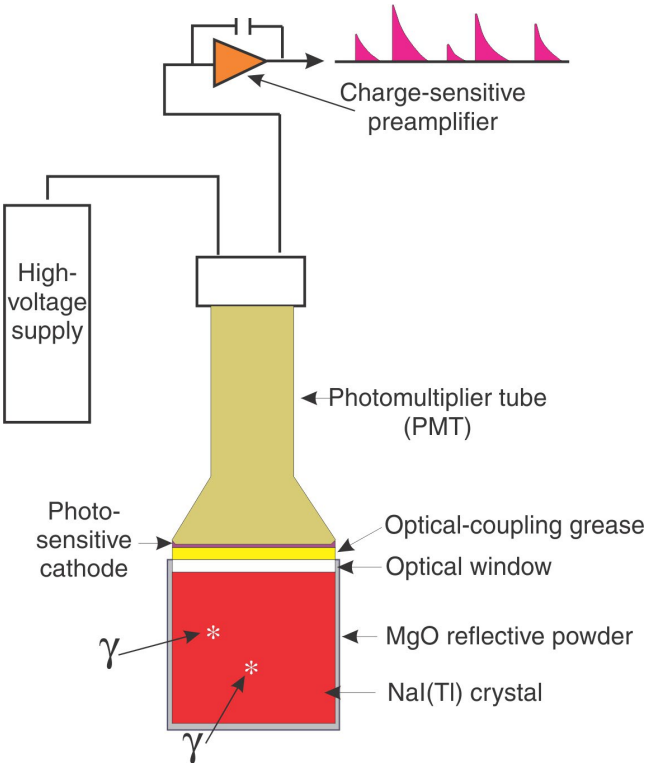

Figure 16. Schematic showing the principal components of a gamma-ray (γ) scintillation detector (*modified from* Bristow, 1979, 1983). MgO = magnesium oxide; NaI(Tl) = sodium iodide (NaI) thallium (Tl) activated crystal.

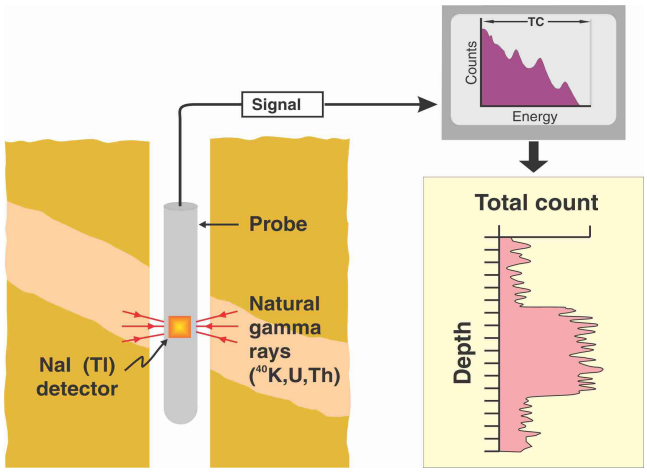

Figure 17. Principle of a total-count gamma-ray logging system. All gamma rays emanating from the three radioelements are counted in one window, generally summed up between 0.1 MeV and 3.0 MeV (MeV = megaelectron volt).

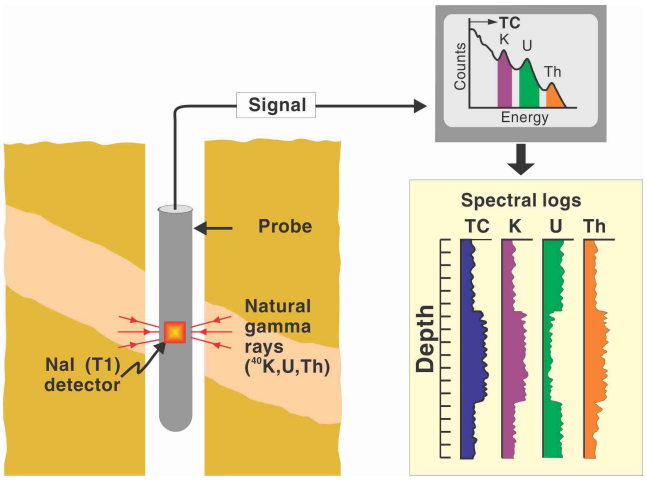

Figure 18. Schematic of measuring principle of a gamma-ray spectral-logging system. Detected gamma rays are sorted into their respective energy to produce a spectrum from 0.1 MeV to 3.0 MeV.

channel. In the logs shown in Figure 18 (processed logs) it is immediately clear that in this case, the source of the high gamma-ray activity in the total-count log is not uranium, but potassium and thorium.

Calibration of total-count gamma-ray logging systems

Before heading out into the field to use a logging system to compute uranium ore grade, it must be calibrated at a calibration facility (for details on calibration facilities *see* 'Gamma-ray probe calibration sites'). There are model holes available that have an ore zone with known concentrations of uranium, thorium, or potassium between barren zones. To calibrate a total-(gross)count system you need only uranium models. Record a log through the ore zone and upper and lower barren zones. Use energies more than 400 keV to minimize the Z effects.

Thick versus thin ore zones

Before going into details about how to calibrate a gamma-ray logging system, it is necessary to look at the detector sample volume and thick versus thin ore zones. Figure 19 shows detectors intersecting a thick (infinite) and thin zone. These two ore zones, a 70 cm and 35 cm thick ore zone, have the same grade. If the detector sample volume is as indicted by the circle, the field of investigation in the 70 cm upper zone is completely within the ore zone. The gamma-ray log reaches a plateau in this zone and the intensity (gamma-ray count rate) in this flat part is proportional to the grade. In the lower 35 cm thick zone, part of the sample volume is in the barren zone when the detector is in the centre. In this thin

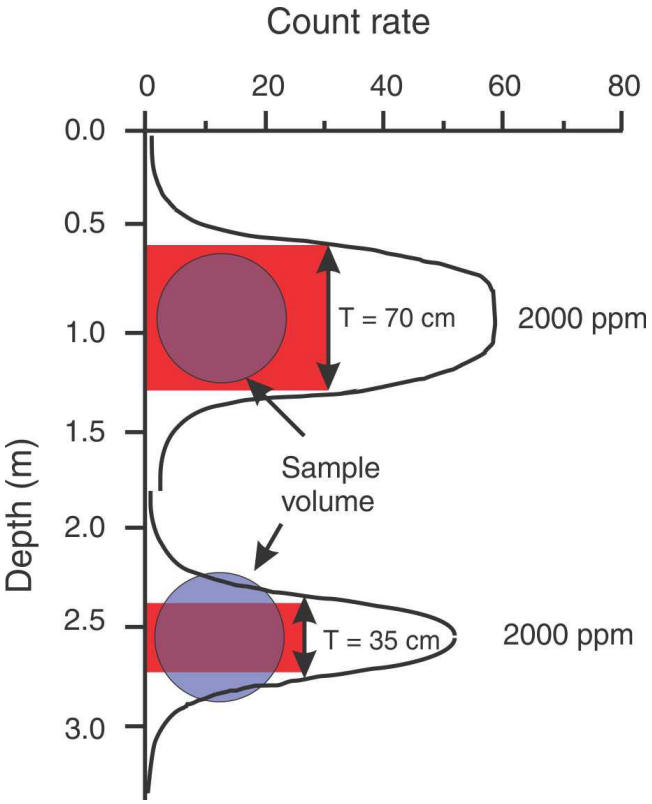

Figure 19. Schematic diagram showing sample volume of detector in a thick and thin zone.

zone, the gamma-ray log does not reach a plateau and the intensity is lower than that observed in the upper zone even though the grade is the same.

The calibration of a total-count gamma-ray logging system requires the determination of the k-factor, sometimes known as the sensitivity. The k-factor is a constant that relates ore grade to the measured gamma-ray intensity. In order to get a more realistic and accurate value for the k-factor, it is important to have measurements made in three models with different grades, plot them, and then compute the slope of this line; this is the k-factor (Fig. 20). For an infinitely thick homogeneous ore zone, the ore grade is computed by multiplying the gamma-ray intensity (or count rate) with the k-factor.

The method just described assumes one is measuring in an infinitely thick zone; however, what happens in a thin zone? In this case one uses what is called the grade thickness product (Fig. 21). Here again, it is better to have measurements in three models with different grades and plot the grade thickness against the area. The k-factor is the slope of the line and given as (grade x thickness)/area.

Measuring the area under the curve from a complex gamma-ray log is tricky (Conaway and Killeen, 1980). The log needs to be digitized over prescribed depth intervals; the area of these intervals is then summed up and this gives the total area (Fig. 22).

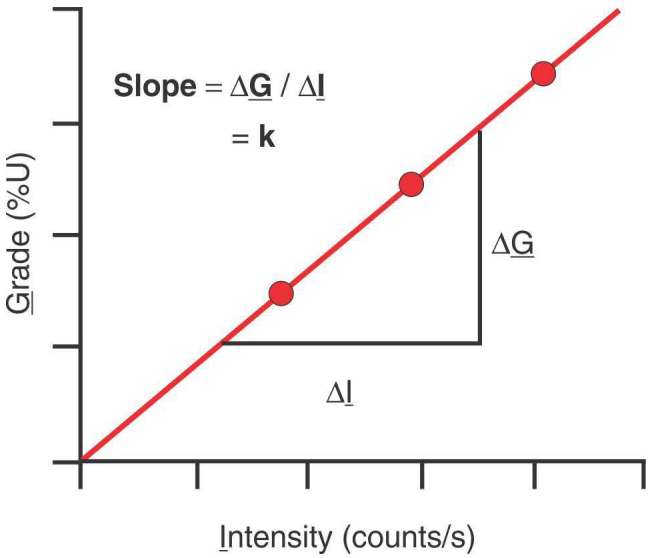

Figure 20. Determination of the k-factor in an infinitely thick zone where the maximum gamma-ray count rate in the centre of the anomaly is proportional to the uranium grade.

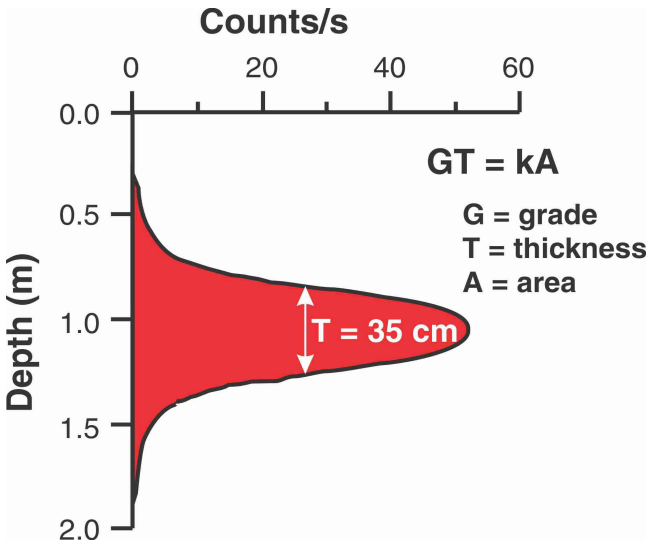

Figure 21. Determining the k-factor for a thin zone.

What happens, however, when one wants to determine the uranium ore grade and thickness in a very complex ore zone? In this case an iterative fitting technique is used (Dodd and Eschliman, 1972). Several layers are generated with approximate grades and a composite anomaly is generated that best fit the real observed anomaly (Fig. 23).

A computer software package is used to do these calculations. It allows one to perform highly accurate nonlinear least-squares curve fitting to multipeak data sets and to calculate the area under each peak. The other method for computing ore grades in a complex ore distribution is to use the deconvolution technique. An in-depth discussion of this

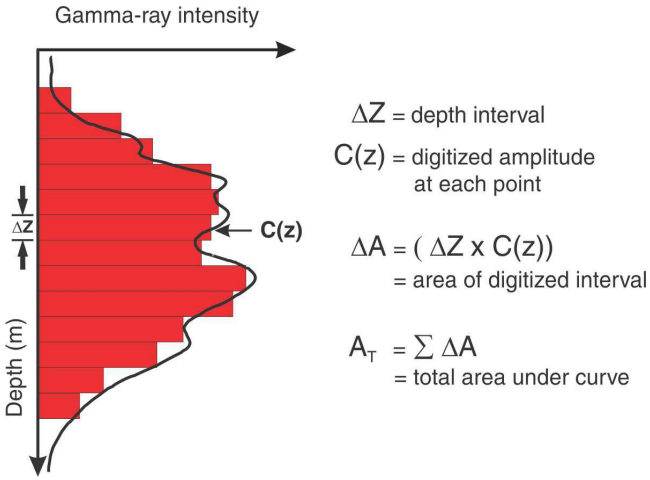

Figure 22. Measuring the area under the curve of a complex gamma-ray log response.

topic can be found in Conaway and Killeen (1978). Now that these basic data-processing methods have been covered, it is possible to focus on the issue of calibration.

Field calibration of a logging system

Logging systems also need to be calibrated in the field. Energy calibration in the field and data acquisition can be done in four steps:

1. Lower probe into the borehole, about 20 m below the water table and temperature stabilize for about 30 minutes for the probe to reach the borehole-fluid temperature.
2. Bring probe quickly to the surface and place a calibration source such as caesium with a gamma-ray energy peak at 661.6 keV. The source should be positioned at the centre of the detector to energy calibrate the system (i.e. adjusting the gain to make sure that the peak from the source is located in the correct channels). Use of just one source assumes energy calibration is linear. To ensure accuracy, more points spread out over a wide energy range are needed. Two sources, caesium with a gamma-ray energy peak at 661.6 keV and yttrium with two gamma-ray peaks at 898.2 keV and 1836.2 keV are usually used. The idea is that the more points used to plot a line, the better the calibration estimate.
3. A one minute spectrum is then recorded with the caesium and yttrium sources on.
4. The probe is then quickly lowered into the borehole and then downhole and uphole logging runs are acquired.
5. Another set of one minute energy calibration spectra are again recorded with the caesium and yttrium sources. The second energy spectra are used to check if there has been any drift during the data acquisition of the downhole and uphole runs.

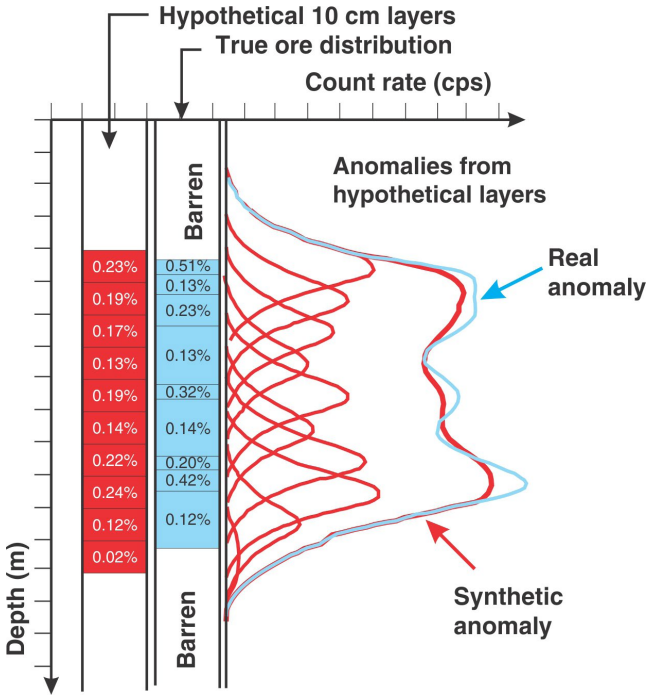

Figure 23. Synthetic anomalies for hypothetical 10 cm layer uranium distribution (*modified from* Dodd and Eschliman, 1972). The grades of the layers are adjusted until the composited anomaly matches the observed real anomaly. Also shown are the true uranium ore-grade distribution and layer thicknesses.

Some gamma-ray probes have internal energy calibration sources instead of the external sources that the GSC has adopted. With an internal energy calibration, one still needs to temperature-stabilize the probe before logging.

Corrections of gamma-ray logging data

After logging data has been acquired in the field, there are several corrections that need to be done before the data can be used because the field conditions will differ from the calibration environment (*see* Killeen et al., 1983; International Atomic Energy Agency, 1986; and Killeen and Elliott, 1990 for detailed discussions of the necessary corrections). The corrections include: dead time, moisture correction, disequilibrium correction, hole size, water correction, casing correction, and Z-effect correction.

Dead time is the difference in time between the actual time at which the data are counted and the time the system takes to process this data. The equation is:

$$N = \frac{R_{obs}}{1 - R_{obs}T}$$

Where N = the corrected count rate

R_{obs} = the observed count rate

T = the dead time of the system

(NB: corrections >50% are unreliable)

The moisture correction (F_m) is done when calibrations are conducted in dry holes and the field holes are saturated. The equation is:

$$F_m = \frac{1-(moisture\ content\ by\ weight,\ calibration\ hole)}{1-(moisture\ content\ by\ weight,\ rock\ formation)}$$

The disequilibrium correction (F_q) must be made as the k-factor is obtained for radioactive equilibrium conditions. If the relative equilibrium is disturbed, the measured gamma-ray activity is no longer indicative of the uranium content of the rocks. A more basic explanation is that the uranium concentration is computed from the gamma-ray count rate of its daughter products (^{214}Bi) and if one or two of the daughter products (e.g. group 2 and 3) between the parent ^{238}U and the ^{214}Bi (Fig. 14) are removed then ^{214}Bi in group 4 will not accurately represent the concentration of the parent ^{238}U. For a given deposit site, the disequilibrium factor is the ratio of the actual amount of uranium (from geochemical assay) to the calculated amount (based on the gamma-ray counts from daughters). There is no disequilibrium if these quantities are equal and the ratio is 1.0; however, if the ratio is less than 1.0, some uranium has been lost and the calculated values will overestimate the quantity of uranium (adapted from International Atomic Energy Agency, 1986). The actual calculation of F_q will not be covered here (*see* Killeen and Carmichael, 1970; Conaway and Killeen, 1978).

The water and hole diameter correction (F_w) must be made as the size of the hole and presence of water in the borehole will reduce the count rate.

The casing correction (F_c) must be made as casing will also reduce the count rate.

The Z-effect correction (F_z) must be made where work is being done in an area with high ore grades and where small or unfiltered detectors are used.

In summary, the calibration equation (adapted from George (2007), Delta Epsilon Calibration White Paper) is:

$$GT = kA$$

$$A = F_w F_c F_m F_q \sum (F_d(R_{obs}) F_z(R_{obs}) R_{obs}) \times \Delta z$$

Where G = grade of ore

T = thickness of ore

k = k-factor or constant of calibration

F_w = water and hole diameter correction factor

F_c = casing correction factor

F_m = moisture correction factor

F_q = disequilibrium correction factor

$F_d(R_{obs})$ = dead time correction factor

$F_z(R_{obs})$ = Z effect correction factor

R_{obs} = observed count rate

Δz = data acquisition interval

How are uranium concentrations reported?

Uranium concentrations are often given in parts per million uranium or per cent uranium. When per cent uranium is used the conversion is:

$$1\ ppm\ U = 10^{-4}\%U = 1.18 \times 10^{-4}\%\ U_3O_8$$

In total- or gross-count gamma-ray logging all the gamma rays are assumed to be coming from uranium. Nice thought, but highly unlikely. As shown previously in Figure 18, gamma rays can also be coming from potassium and thorium. This is where a gamma-ray spectral logging system is needed.

Gamma-ray spectrometry

Gamma-ray spectrometry reveals the source of the gamma rays being measured. Figures 24, 25, and 26 show the line spectra and model borehole spectra from potassium, uranium, and thorium, respectively. The isotope used for potassium is ^{40}K with gamma-ray energy of 1460 keV (Fig. 24a) and therefore, the energy window is set between 1360 keV and 1560 keV (Fig. 24b) to monitor gamma rays from ^{40}K. Uranium has a number of gamma-ray emitters in its decay series, so there is a choice of looking at several peaks to determine uranium concentration (Fig. 25a). Usually, gamma rays from bismuth-214 are used. Its gamma-ray energy is 1760 keV and can be found in the 1610–2300 keV energy window (Fig. 25b). Thorium also has several gamma-ray emitters in it decay series. There is a well isolated thallium-208 peak at 2615 keV and the energy window to monitor Th is set between 2400–3000 keV (Fig. 26b). In contrast, the total- or gross-count window is a wide one, 400–3000 keV (Table 3).

Stripping ratios

Figure 27 is a composite of gamma-ray spectra from the potassium, uranium, and thorium model boreholes from the Bells Corners gamma-ray calibration facilities and shows the K-, U-, and Th-spectral window locations as discussed above. Notice when looking at the potassium window, a significant number of gamma rays from uranium and thorium are also being picked up. In the uranium window, a very small amount of potassium is present and a large number of gamma rays from thorium. Similarly, in the thorium window there are practically zero potassium counts, but still some counts from uranium. Therefore, a way to separate these out is needed.

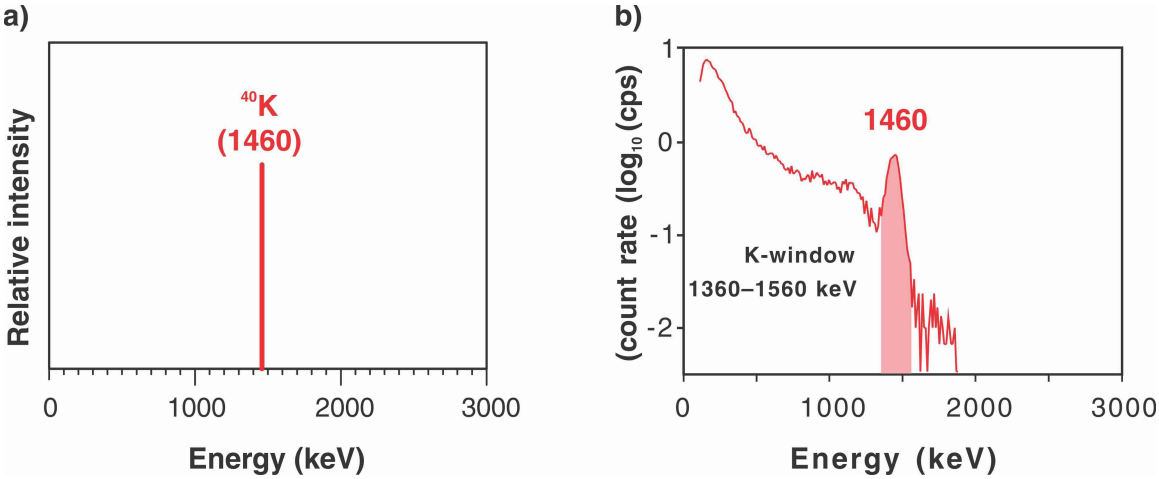

Figure 24. a) Gamma-ray emission line spectra of potassium; **b)** potassium spectra recorded with a NaI(Tl) detector in a postassium model borehole at the Bells Corners calibration facilities in Ottawa, Ontario.

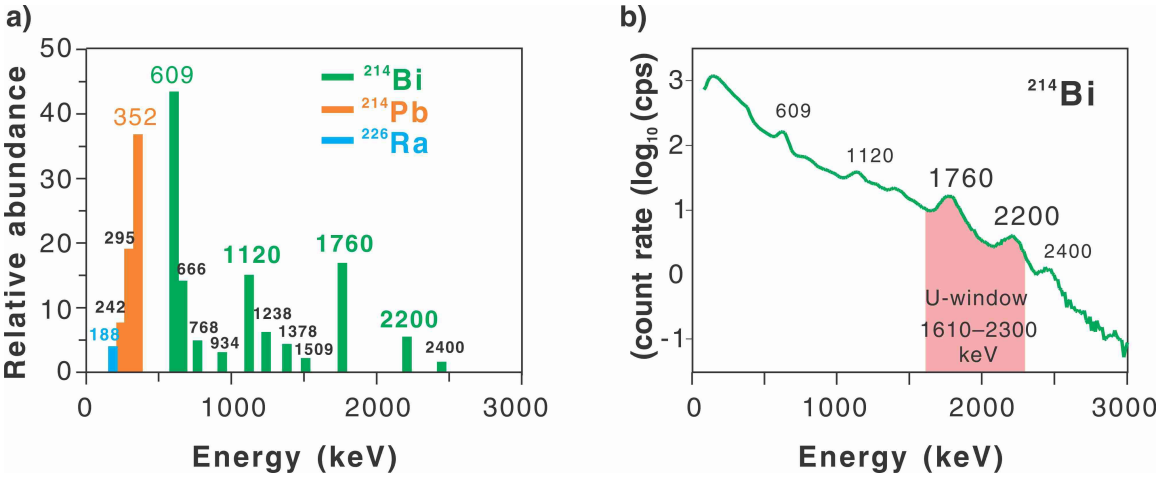

Figure 25. a) Gamma-ray emission line spectra of uranium; **b)** uranium spectra recorded with a NaI(Tl) detector in a uranium model borehole at the Bells Corners calibration facilities in Ottawa, Ontario. A wide energy window (GSC logging system) is set between 1610 KeV and 2300 KeV, encompassing two ^{214}Bi peaks.

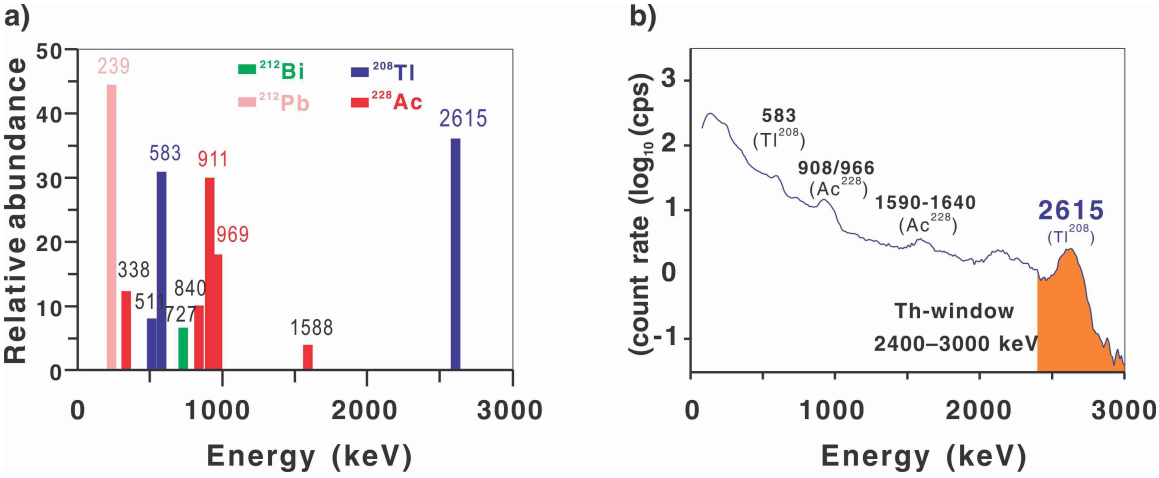

Figure 26. a) Gamma-ray emission line spectra of thorium with peaks for ^{212}Bi, ^{212}Pb, ^{228}Ac, and ^{208}Tl daughter products; **b)** thorium spectra recorded with a NaI(Tl) detector in a thorium model borehole at the Bells Corners calibration facilities in Ottawa, Ontario. The Th energy window is set between 2400 keV and 3000 keV at the ^{208}Tl peak.

Table 3. Spectral gamma-ray windows.

Window name	Isotope used	Gamma-ray energy peak	Energy window (keV)
Potassium	^{40}K	1460	1360–1560
Uranium	^{214}Bi	1760	1610–2300
Thorium	^{208}Tl	2615	2400–3000
Total count			400–3000

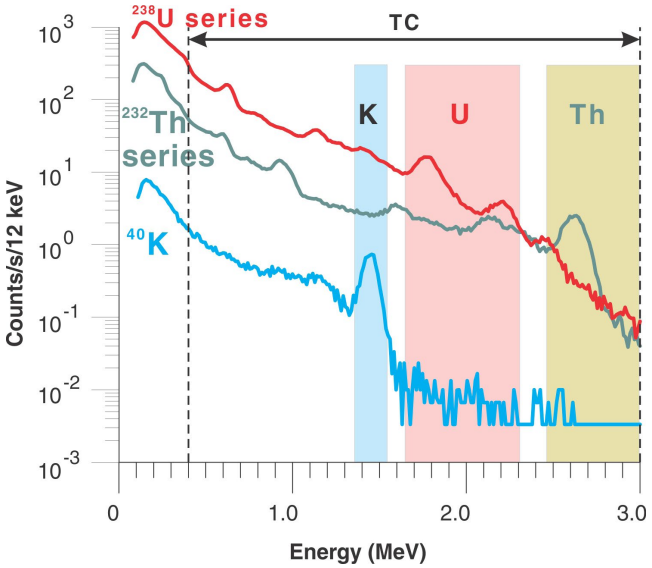

Figure 27. A composite of gamma-ray spectra from the potassium, uranium, and thorium model boreholes from the Bells Corners calibration facilities, Ottawa, Ontario.

The following equations (simplified, assuming stripping ratios, g and b to be zero) are used to get the corrected count rate for each radioelement alone (Grasty, 1977; Killeen, 1983).

$$\mathrm{Th}_s = \frac{Th - aU}{D}$$

$$\mathrm{U}_s = \frac{U - \alpha Th}{D}$$

$$\mathrm{K}_s = \frac{(\alpha\gamma - \beta)Th + (\alpha\beta - \gamma)U + (1 - a\alpha)K}{D}$$

$$D = 1\text{-}a\,\alpha$$

Where, α, β, γ, a, b, g are the stripping ratios:

α is used to strip off Th gamma rays in U-window,

β is used to strip off Th gamma rays in K-window,

γ is used to strip off U gamma rays in K-window,

a is used to strip off U gamma rays in Th-window,

b is used to strip off K gamma rays in Th-window,

g is used to strip off K gamma rays in U-window.

The b and g stripping factors are virtually zero (*see* Fig. 28) and a is usually very small.

The Th, U, and K are raw gamma-ray count rates recorded in thorium, uranium, and potassium windows, respectively, in counts per second. The Th_s, U_s, and K_s are stripped (corrected) gamma-ray count rates in those same windows.

Figure 29 shows raw data on the left and processed or stripped data on the right. The high total gamma-ray count near the top of the hole is due to high potassium content. When one takes a close look at the raw uranium log, one sees an anomalously high count rate near the bottom of the hole and it appears as if there is a significant amount of uranium present; however, after stripping, it is obvious that there is no uranium in this zone. The high count in the raw uranium log is actually from the backscattered gamma rays from thorium.

Calibration of gamma-ray spectral logging systems

Gamma-ray spectrometry systems also need to be calibrated to get the ore grade or determine the radioelement concentration. The first step involves a visit to a calibration facility with K, U, and Th models. Record a log with the system being used through the ore zone and the barren zones (upper and lower). Then compute the stripping factors (as discussed above) and sensitivities or k-factors. Table 4 shows the standard calibration conditions for three major international calibration facilities. Table 5 provides a comparison of assigned and calculated uranium grades for these same sites.

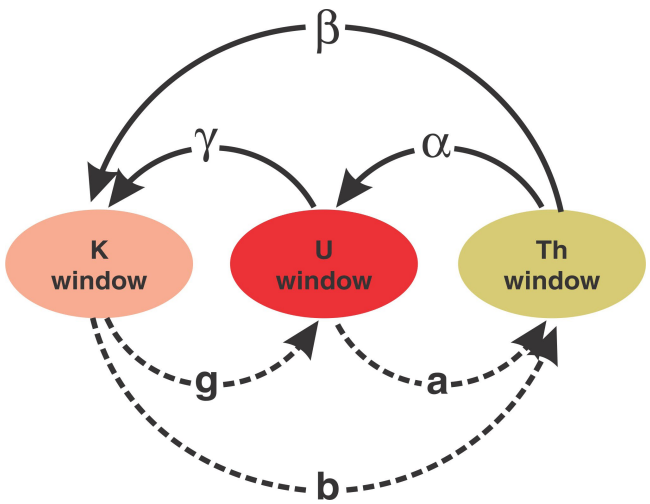

Figure 28. Schematic showing the gamma-ray interaction between the K, U, and Th energy windows and the stripping factors that are used to correct for these interferences. The arrows indicate the gamma rays detected in an energy window that are not related to the radioelement being monitored (e.g. the arrow for β indicate gamma rays observed in the K-window that are originating from Th).

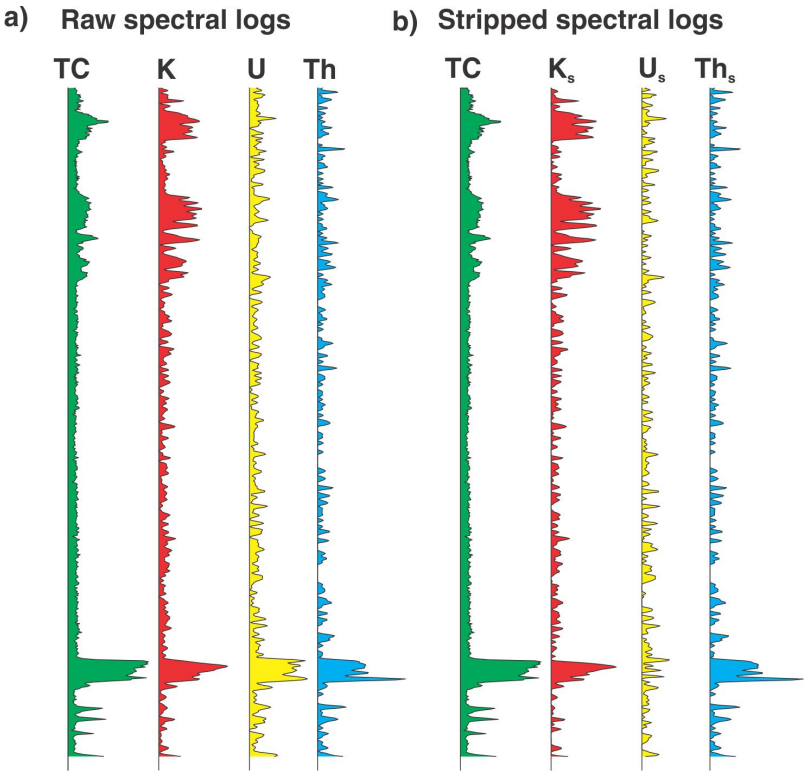

Figure 29. Natural gamma-ray spectral logs: **a)** raw logs, **b)** stripped logs. TC = total count.

Table 4. Standard calibration conditions for three international calibration facilities (Killeen et al., 1983).

Model	BU-6	N3	AM-1
Location	Ottawa, Canada	Grand Junction, United States	Adelaide, Australia
Ore zone thickness (m)	1.48	1.28	1.41
eU_3O_8 grade (ppm)	1160	2400	2090
$eThO_2$ (ppm)	5	-----	10
K (%)	0.26	-----	0.76
Wet density (g/cm^3)	2.405	2.09	2.31
Dry density (g/cm^3)	2.289	1.83	2.14
Moisture (%)	4.8	12.3	7.4
Porosity (%)	11.7	-----	17
Borehole diameter (mm)	60	114	108
Borehole fluid	Water*	Air*	Air*
Borehole casing	None	None	None

* = Standard borehole fluid conditions
----- = No data

Table 5. Comparison of assigned and calculated grades for the Canada, U.S.A., and Australia standard calibration models.

Model borehole	Assigned grades (eU_3O_8, ppm)	Relative assigned grades	Relative measured grades	Calculated grades (eU_3O_8, ppm)
BU-6	1160	1.000	1.000	1160
N3	2400	2.069	1.883	2184
AM-1	2090	1.802	1.911	2216

The following relationships are used to compute the ore grades from spectral logs:

$G_K T = C_K A_K$, for potassium

$G_U T = C_U A_U$, for uranium

$G_{Th} T = C_{Th} A_{Th}$, for thorium

Where G = grade

T = thickness

C = c-factor equivalent to the k-factor in total count

A = window count area

The subscript refers to the radioelement being analyzed.

OTHER BOREHOLE GEOPHYSICAL METHODS

Introduction

When a discussion on uranium logging comes up, most people automatically think of gamma-ray logging, but there are other geophysical methods that can also be used in uranium exploration. Some of the most familiar ones are electrical, acoustic, density, and temperature. In addition there are some less common and even 'exotic' ones that will be mentioned briefly at the end of this section.

Now, these other methods will not detect uranium directly and will not provide any information on the grade or the quantity; however, if one drills and misses the deposit, these methods will indicate if there is something close by. They do this by identifying the geology that hosts uranium and detecting structures or alteration that have been shown to be associated with uranium deposits.

Electrical methods

Three common electrical methods are induced polarization (IP), resistivity, and self potential (SP). Figure 30 is a schematic of a resistivity-IP-SP logging system. There is an electrode system in the borehole, a depth counter to indicate where a measurement is being made, a winch to move the probe up and down the hole, a transmitter to supply current to the electrodes, and a data-acquisition system to record, display, and store the data. This tool usually includes a downhole current electrode and two downhole potential electrodes. Another return current electrode is positioned on the surface. Measurements can be made in the frequency or time domain. In the time domain, a square wave current with an 'off' time between positive and negative parts of the waveform is transmitted. Current waveform durations may vary from 1.0 s to 8.0 s. Resistivities are computed from potential measurements made during the ON transmission time of the current waveform. These electrical measurements are only possible in water-filled, open holes. They cannot be made in plastic- and/or steel-cased holes or in dry holes. A detailed description of the resistivity-IP logging system can be found in Mwenifumbo (1990).

Resistivity

Resistivity is a method that works by measuring the electrical resistivity of a rock and using this information as a basis for identifying the rock type. Resistivity is a fundamental property that measures how strongly a material opposes the flow of electrical current. Most rock materials are poor conductors and their resistivities are governed primarily by their porosity, degree of fracturing, salinity of the pore water, degree of saturation of the pore spaces, and to a lesser extent by the intrinsic minerals that constitute the rock.

Figure 31 shows some reference data on resistivities of various rock types. Notice that a very low resistivity indicates a sulphide or graphite zone. If the focus is on granite, altered granite bodies have lower resistivities than unaltered ones because of porosity increase and the presence of conductive alteration minerals such as clay.

Two additional applications of resistivity data are model testing and ground-truthing. Model testing is confirming a proposed model with actual data from the site to see if ground or airborne methods are going to work in a particular area. To determine this, modelling needs to be done. Rock-property data from well logging are used to make the models.

Ground-truthing is using logging data to increase confidence in your data interpretation from other data you have collected. The borehole data give a quantitative basis for interpretation.

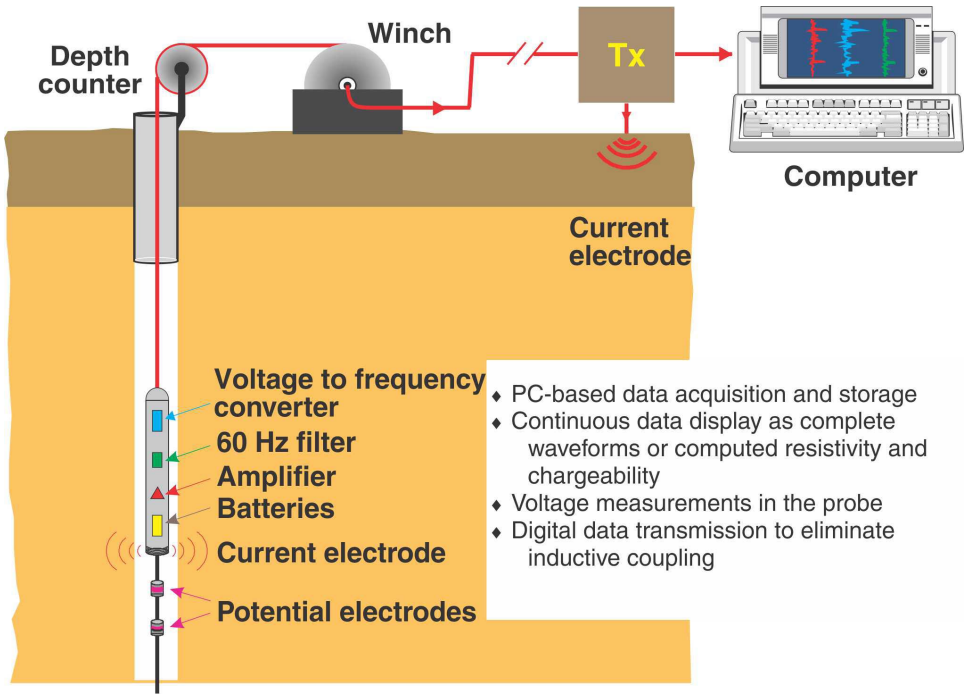

Figure 30. Schematic of the induced polarization and resistivity logging system.

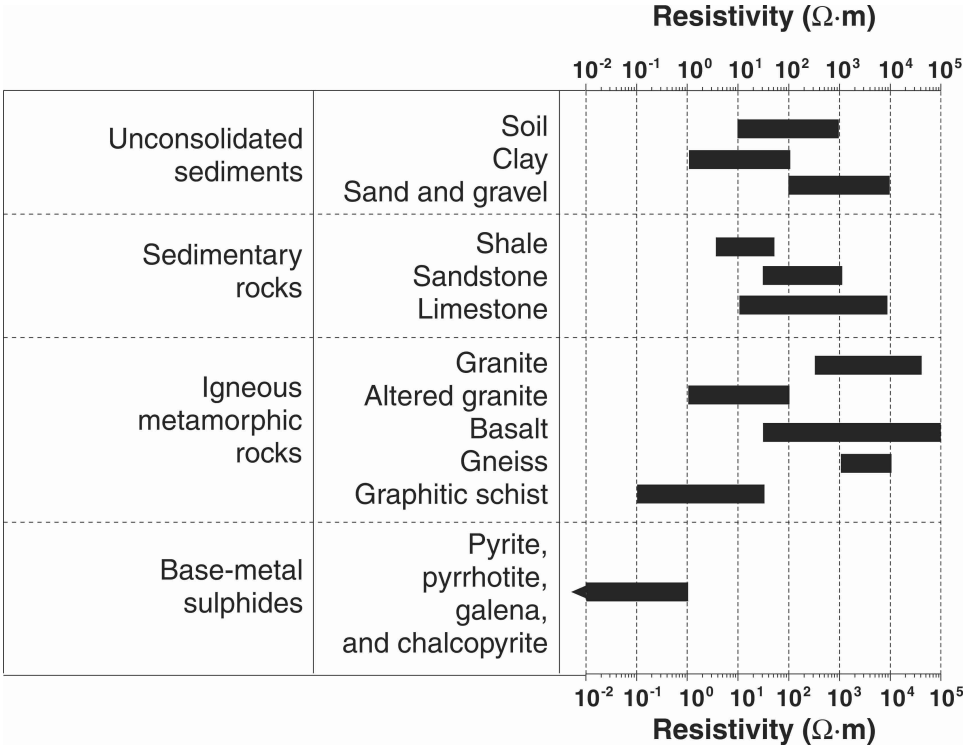

Figure 31. Approximate ranges of resistivities of some of the major rock types and base-metal sulphide minerals.

Induced polarization

Induced polarization (IP) is another electrical borehole geophysical method used to characterize material below the surface. An electric current is injected into the ground through two electrodes and the voltage is picked up by two other electrodes. For the time-domain IP system, a constant current is transmitted for a given period and then turned off. The process is repeated with the current polarity changed (a negative current on). The potential observed when the current is on gives the resistivity measurements and the data collected while the current is off gives the IP measurements. The ratio of the secondary voltage measured during the current-off time to the primary voltage measured during the current-on time is related to the electrical polarizability of the rock and is called chargeability. A high chargeability response is an indication of the presence of disseminated metallic sulphide and oxide minerals, graphite, or cation-rich clay minerals such as illite and montmorillonite (Mwenifumbo, 1990). One of the major alteration processes within a number of mineral deposits including uranium is limonite and/or hematite and/or pyrite and this is a target for most IP logging applications aimed at vectoring in toward blind deposits (missed during drilling).

Self potential or spontaneous potential

The self potential or spontaneous potential (SP) method measures the naturally occurring electrical potentials. Large self potentials observed within and around base-metal sulphide and graphite bodies are mainly caused by electrochemical processes (Sato and Mooney, 1960; Hovdan and Bolviken, 1985). Low-resistivity anomalies correlating with SP and IP anomalies are therefore good indications of the presence of conductive minerals.

What do resistivity and IP data look like?

Figure 32 shows resistivity and IP data from the Athabasca Basin. In sedimentary rocks, the resistivity log is frequently used to map changes associated with variations in porosity. Some alteration processes such as silicification tend to reduce the porosity and hence increase the resistivity of the rocks. High resistivity in the bottom of the Bird Member of the Manitou Falls Formation (MFb) and in the Read Formation between 450 m and 600 m is due to silicification. Here the high IP is due to the presence of iron-oxide minerals like hematite. This indicates that even though no mineralization has been intersected, a mineralized zone is near. Desilicification results in lower resistivities as seen between 250 m and 450 m. The high resistivity in the Dunlop Member of the Manitou Falls Formation (MFd) is associated with clay alteration and there is an increase in kaolinite and dravite.

In igneous and metamorphic rocks, the resistivity log is useful mainly in mapping conductive minerals and fracture zones. Figure 33 shows gamma-ray, resistivity, and IP logs collected at McArthur River in Athabasca Basin. Resistivity and IP were used to identify some graphitic conductors in the basement below 575 m.

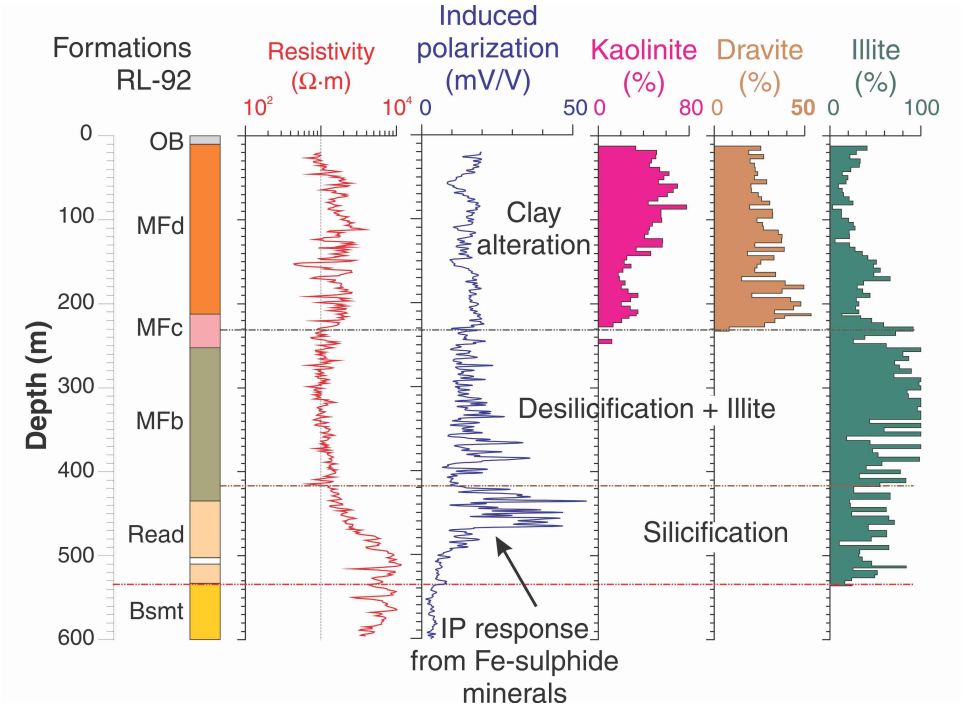

Figure 32. Resistivity, IP, and logs of alteration minerals (kaolinite, dravite, and illite from PIMA (portable infrared mineral analyzer) measurements) showing the electrical response of these alteration minerals. OB = overburden; MFd = Manitou Falls Formation, Dunlop Member, MFc = Manitou Falls Formation, Collins Member; MFb = Manitou Falls Formation, Bird Member; Read = Read Formation; Bsmt = basement.

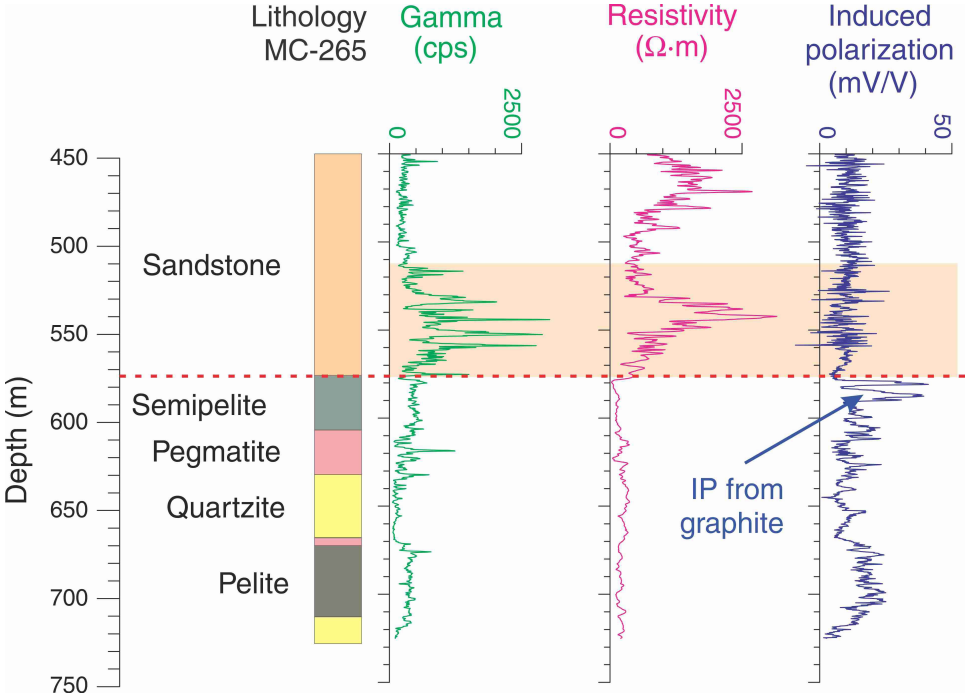

Figure 33. Gamma-ray, resistivity, and induced polarization near the bottom of the hole at the contact between the sandstone and basement rocks. The semipelite and pelite units are graphitic and show an increase in the IP response.

Inductive conductivity

Inductive conductivity (EM) loggers do not require contact with the formation or fluid in the borehole; hence, they are commonly used in plastic-cased, and/or dry boreholes (the method does not work in steel casing). A high-frequency electromagnetic signal is transmitted from, and received by, two coils in the probe. The magnitude of the induced electromagnetic field (the so-called out-of-phase response) is proportional to formation electrical conductivity (at relatively low conductivities). The necessary spacing between the transmission and receiving coils in the probe results in the observed conductivity being the average of a large volume of material around the probe, the extent of which is governed by the intercoil spacing; hence, a form of smoothing (some correction factors applied) is imposed on the conductivity log. As well, most induction logging probes have been designed to be relatively insensitive to near effects (such as change in hole size or saline drilling fluids), and most of the conductivity response comes from 15–100 cm out from the tool. Further details can be found in Taylor et al. (1989). Figure 34 shows gamma-ray and inductive conductivity logs. Uranium is usually associated with conductive graphitic structures. There are high conductive responses seen in the conductivity log just above the bottom uranium ore zone. Also, pyrite and some other sulphide minerals are associated with uranium mineralization. Notice the high conductivity of the niccolite (a nickel arsenide, NiAs) above the upper uranium ore horizon in this hole.

Full-waveform acoustic (sonic) logs

In acoustic logging, a transmitter located in the borehole emits a pulse of mechanical energy that is recorded by one or more receivers located in the borehole some distance away from the transmitter (Fig. 35). In full-waveform acoustic logging, the complete acoustic wave at each receiver is recorded digitally. The character of the acoustic signal that is detected by the receivers is affected by, among other things, the mechanical properties of the rock around the borehole.

How does it work?

The probe contains a single transmitter at the base of the probe and two receivers located above the transmitter (Fig. 36).

A compressional (P) wave is generated in the borehole fluid by pulsing of the transmitter (Tx). P-waves are characterized by pressure oscillations that are parallel to the direction of propagation. Liquids can only support P-waves; however, solids can support both P-waves and shear waves (S-waves, in which the oscillations are perpendicular to the direction of propagation). The P-wave generated in the borehole radiates away from the transmitter in all directions. At the borehole wall, acoustic energy is reflected back into the borehole and refracted into the rock. Because solids can support both P-waves and S-waves, some of the acoustic energy that is refracted into the rock is converted to S-waves.

Some of the energy that strikes the wall at the critical angle for P-waves (determined by the P-wave velocities in the rock and borehole fluid) will propagate as a P-wave along the borehole wall. Likewise, some of the energy that

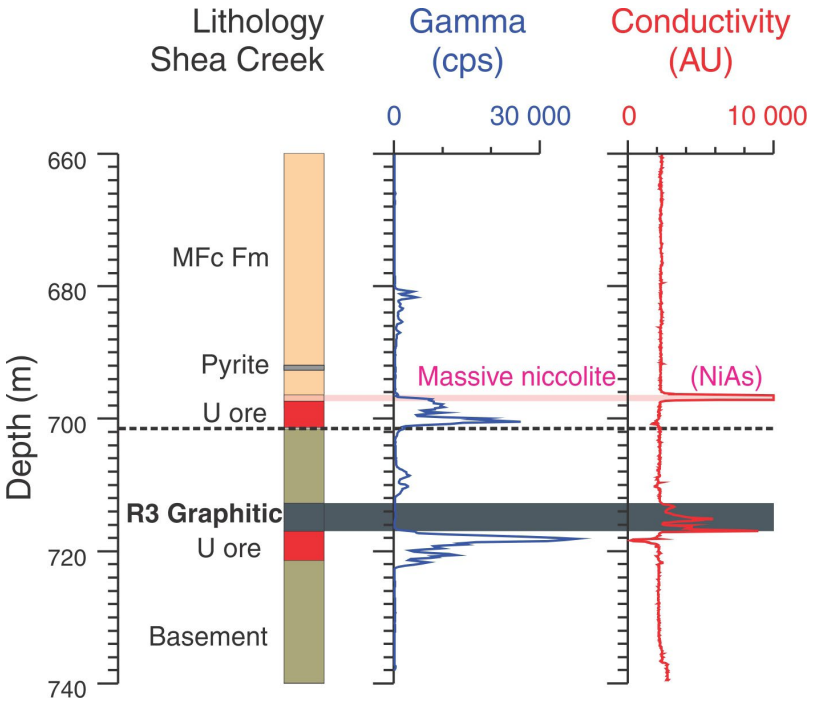

Figure 34. Gamma-ray and conductivity response at the Shea Creek deposit, Saskatchewan. The conductivity data are in arbitrary units (probe not calibrated). Uranium mineralization is closely associated with the R3 graphitic conductor that shows high conductivity above the lower uranium ore horizon. There is an extremely high-conductivity anomaly at the upper contact of the upper uranium mineralization that is due to the presence of massive niccolite.

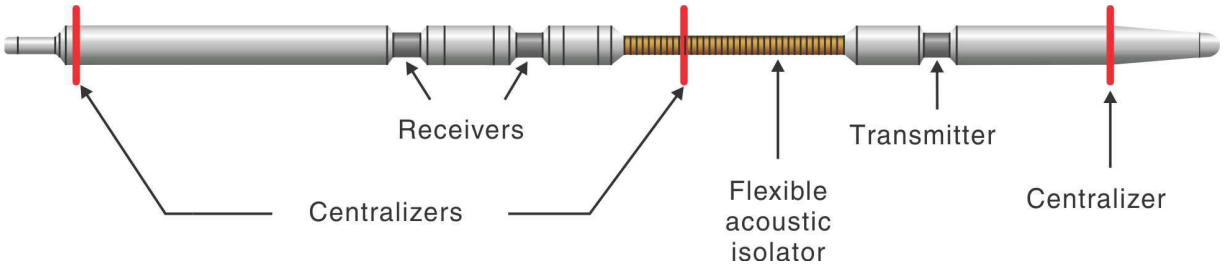

Figure 35. Two-receiver, one-transmitter full-waveform sonic probe.

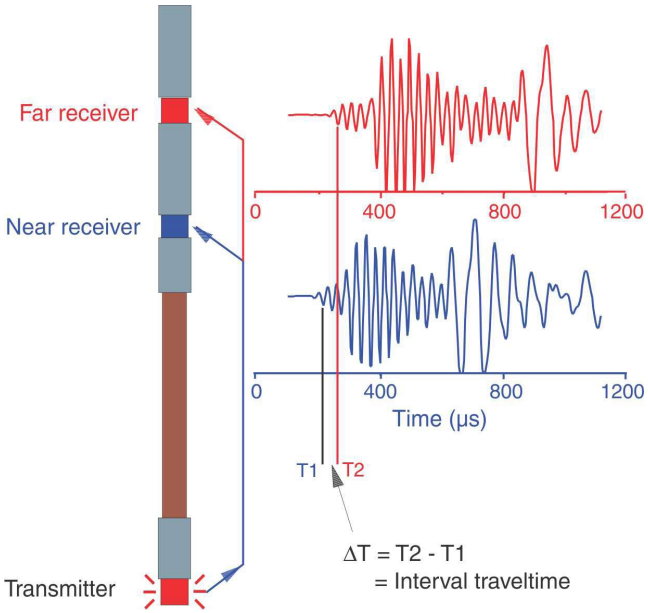

Figure 36. Typical full-waveform signal recorded at the two receivers. The ΔT is the interval traveltime between the two receivers from which the interval compressional-wave velocity is computed.

strikes the wall at the critical angle for S-waves (determined by the S-wave velocity in the rock and the P-wave velocity in the fluid) will propagate as an S-wave along the borehole wall. As these P- and S-waves travel along the borehole wall, energy is reradiated back into the borehole at the critical angles as P-waves. The energy that is reradiated back into the borehole is detected at the receivers.

A third type of wave is the tube wave (or Stoneley-type acoustic wave), which has a wavelength in excess of five times the diameter of the borehole. The velocity of tube waves is less than that of the P-wave in fluid or the S-wave in the solid.

Thus, acoustic logging probes with two receivers, record the traveltime between receivers divided by the receiver separation (the 'interval traveltime') in units of microseconds per foot.

The P-wave through the rock arrives at the receivers first and is known as the 'first arrival'. The interval traveltime that is recorded by acoustic logging systems corresponds to this first arrival. Two common sources of error in the interval traveltime computed this way are caused by cycle skipping and noise. Both errors tend to cause spikes in the interval traveltime log.

Acoustic logging requires water-filled boreholes to make good 'contact' with the surrounding rock. Full-waveform acoustic logging is generally done in open (uncased) holes; however, it is possible to determine P- and S-wave velocities in cased holes.

The depth of penetration in acoustic logging is about one wavelength, which is a function of source frequency and acoustic velocity. Typical source frequencies cover the range of about 10–30 kHz and P-wave velocities in hard rocks usually fall in the range of 5–8 km/s. The depth of penetration for P-waves for this tool is about 20 cm in hard rocks.

For more details on full-waveform acoustic logging, consult Paillet and Cheng (1991) and Paillet et al. (1992).

What drillhole environment is required?

From the above discussion it is clear that acoustic logging requires open, water-filled holes; however, it can and has been done in plastic-cased holes if the probe is kept in contact with the wall.

What are the applications?

Full-waveform acoustic logs are used in mapping structure and alteration and have many applications. They are useful in the interpretation of hole-to-hole seismic tomography and surface seismic data (Fig. 37).

Acoustic logs can also be used to determine porosity in porous rocks (Paillet and Cheng, 1991), in the detection of fractures, and the measurement of fracture permeability, and are useful in hole-to-hole lithological correlation (i.e. model testing and ground-truthing). These applications are found in Figure 38.

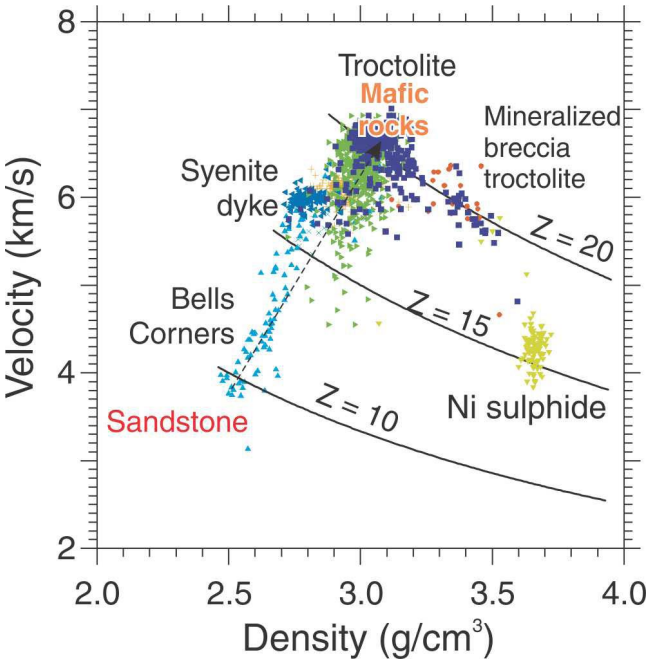

Figure 37. Velocity-density crossplot with acoustic impedance, Z. The normal relationship between velocity and density is that velocity increases with increase in density. This relationship, however, does not hold for base-metal sulphide minerals especially nickel-sulphide minerals.

Figure 39 gives typical P-(compressional)wave velocities in some rocks and minerals (Pflug et al., 1994). The different colours indicate there is a range found for these materials depending on the source of the data. This variability can be due to differences in compaction, porosity, etc. For example, cemented rock is often found in high-grade uranium situations and soft, porous rock is often found in low-grade uranium situations. The highly cemented rock transmits the waves better.

What do the data look like?

The lithology, velocity of P-waves, tube-wave amplitude, and full-waveform acoustic logs for a hole in the Athabasca Basin are presented in Figure 40. This is an example of sonic logs being used to map structures. Notice the low velocities and low tube-wave amplitudes in the fault zones (e.g. at 200 m and 520 m). Both the P-wave velocity and tube-wave amplitude logs show a highly fractured Manitou Falls Formation, Dunlop Member (MFd, 40–130 m) and Read Formation.

An example of acoustic logs used to map alteration is found in Figure 41. Lithology, resistivity (*see* 'What do resistivity and IP data look like?'), and velocity of the P-wave logs show characteristic alteration signatures. Silicified zones

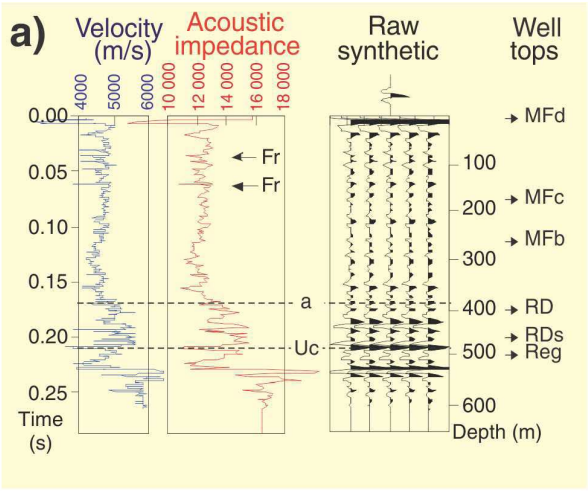

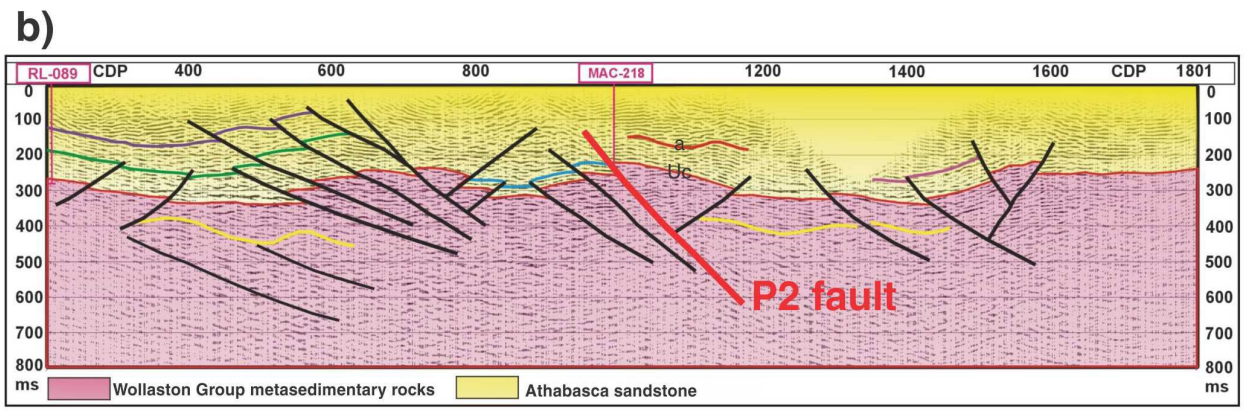

Figure 38. Applications of sonic logging, including **a)** model testing, and **b)** ground-truthing (*modified from* Györfi et al., 2002). The synthetics generated from the sonic logs indicate that one should be seeing reflectors in the silicified sandstone units (Fig. 38a) and at the unconformity (Uc). The processed seismic data (Fig. 38b) show these reflectors. MFd = Manitou Falls Formation, Dunlop Member; MFc = Manitou Falls Formation, Collins Member; MFb = Manitou Falls Formation, Bird Member; RD = Read Formation; RDs Read Formation, seismically differentiated; Reg = regolith; Fr = fracture zone; a = alteration

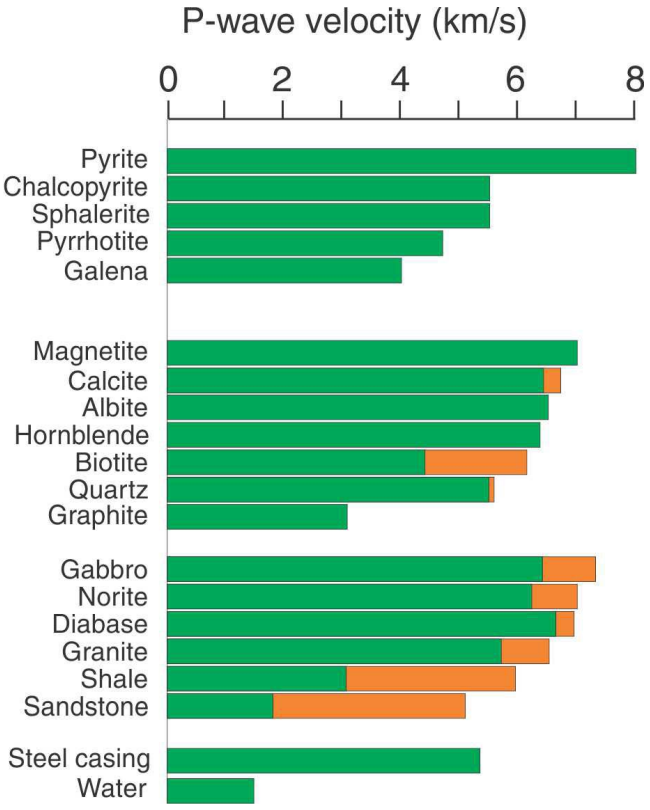

Figure 39. Typical velocities of some minerals and rocks (Pflug et al., 1994).

have higher velocities compared to unsilicified zones. This is also correlated with high resistivity. Fracture zones show low velocities because of increased porosity.

A final caution

Acoustic logging systems are complex. Both a trained operator to collect good quality data and a trained geophysicist to process and interpret the data are required. Figure 42 shows the raw and processed version of an acoustic velocity log and it should be clear why a high level of expertise is required.

Density (gamma-gamma density)

The overall density of a rock includes the solid matrix and the fluid enclosed in pores. Geologically, bulk density is a function of the density of the minerals forming a rock (i.e. matrix) and the enclosed volume of free fluids (i.e. porosity).

On the left in Figure 43 is a schematic of a borehole density probe. The source emits gamma rays that travel through the formation and are detected by a gamma-ray detector. This is the same detector that was discussed in 'Introduction' in 'Gamma-ray and spectral gamma-ray logging'. The number of gamma rays detected depends on the density of the materials they pass through. On the right side of the figure are typical data recorded by a density system. Notice there is a low-energy window (LEW) and a high-energy window

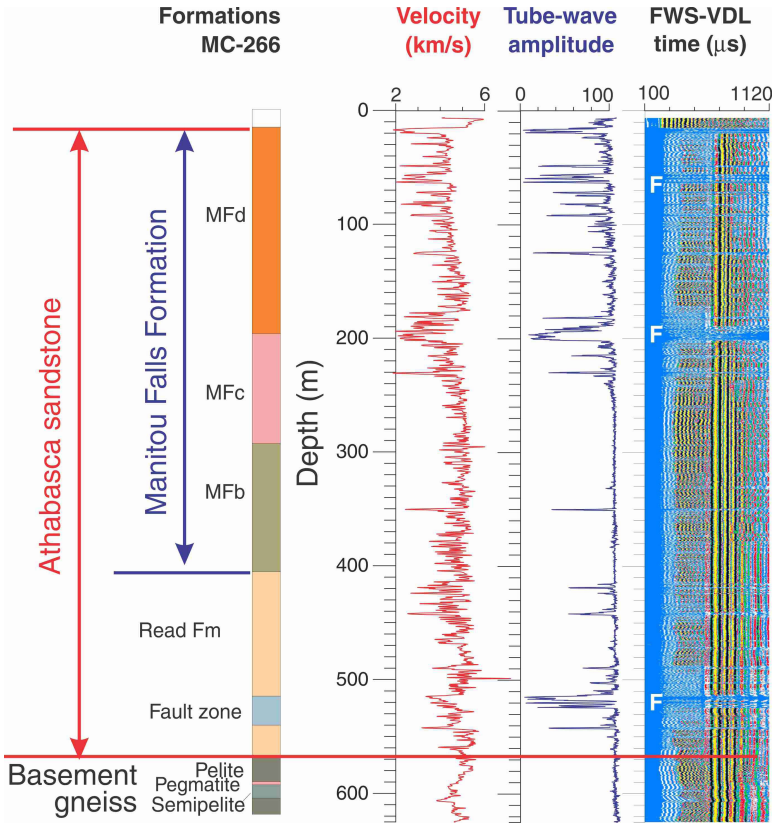

Figure 40. Lithology, p-wave velocity, and tube-wave amplitude logs acquired at McArthur River deposit, Athabasca Basin. The logs indicate three major fracture zones (F) in the Athabasca Basin sandstone units; around 60 m, 200 m, and 520 m. These fault zones may be associated with the P2 fault. MFd = Manitou Falls; Dunlop Member, MFc = Manitou Falls Formation, Collins member, MFb = Manitou Falls Formation, Bird Member; F = fracture zone; FWS-VDL = Full-waveform sonic variable density log.

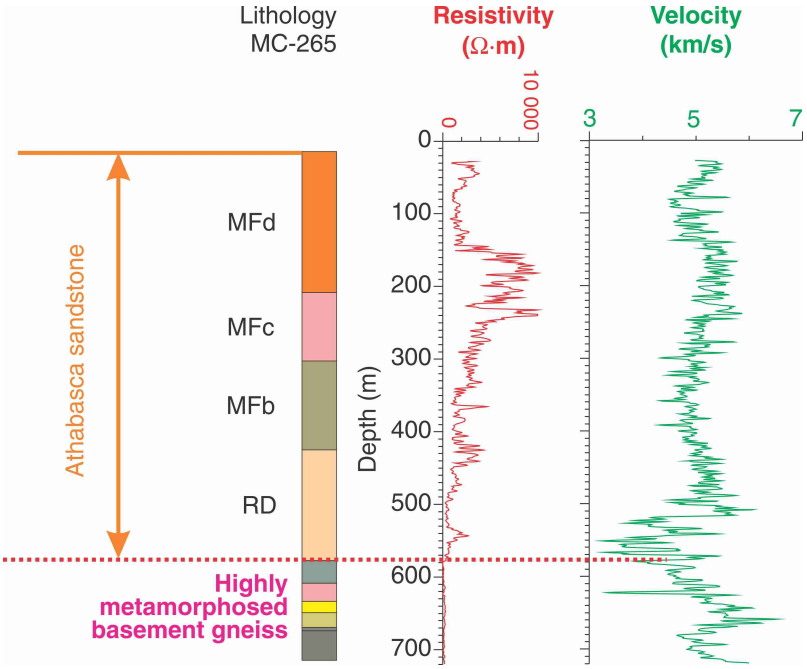

Figure 41. Resistivity and p-wave velocity logs intersecting highly silicified sandstone units; have high resistivity and high velocity (150–250 m). The velocity log shows a highly fractured bottom section of the Read Formation (RD) and the top of the basement rocks. The resistivities are very low in the graphitic basement gneiss. MFd = Manitou Falls Formation, Dunlop Member, MFc = Manitou Falls Formation, Collins Member, MFb = Manitou Falls Formation, Bird Member.

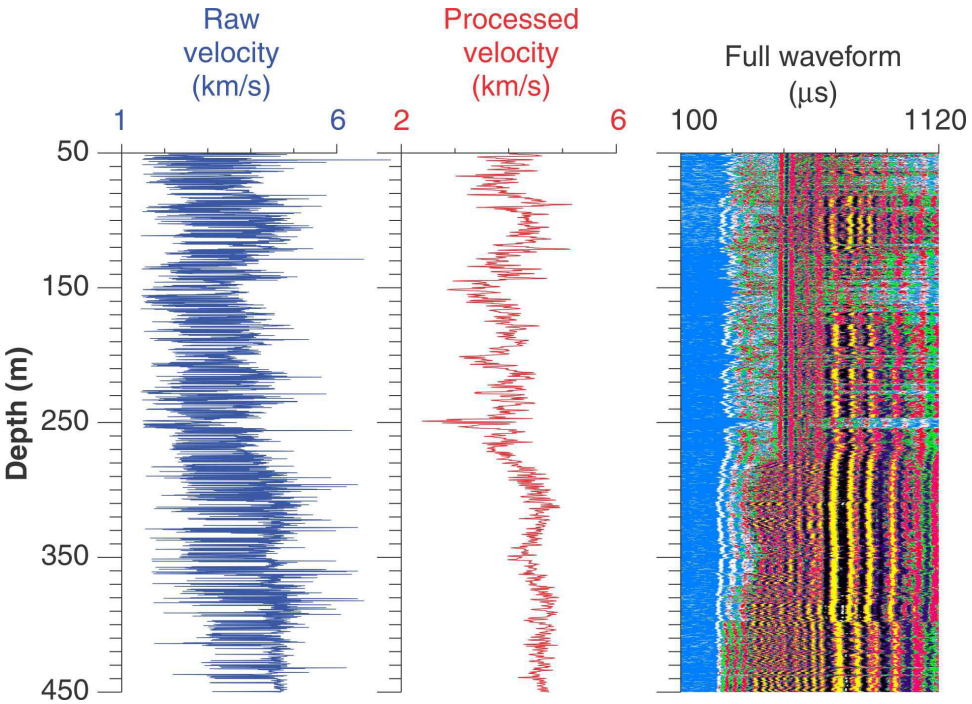

Figure 42. Raw p-wave velocity determined using an automatic p-wave velocity–picking algorithm and the reprocessed velocity. Note how noisy the raw log is that would have been presented from an untrained interpreter.

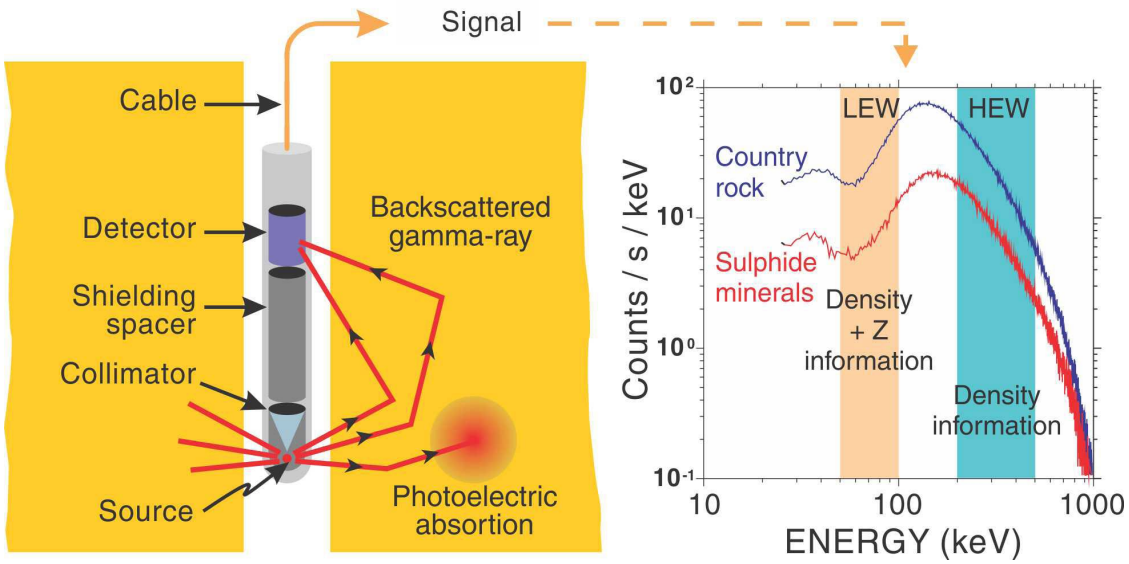

Figure 43. Schematic figure showing a spectral gamma-gamma density probe and the typical backscattered gamma-ray spectra that would be acquired through low-density–low-effective-atomic-number country rock and through high-density–high-atomic-number sulphide minerals.

(HEW). The density data are derived from the readings in these windows. Information about the elemental composition or heavy-element content in the formation can be derived from the ratio of the count rates in the two energy windows. The ratio increases when the probe passes through zones containing heavy elements. Thus the log can be considered as a heavy-element indicator, and can be calibrated in some conditions to produce an assay tool for quantitative determination of the heavy-element concentration in situ along the borehole, without resorting to chemical analysis of the core (Killeen and Mwenifumbo, 1988).

Acoustic impedance (Z) of a material is defined as the product of its density (ρ) and acoustic velocity (V).

$Z = \rho \times V$

Where,

Z = acoustic impedance of material (Ns/m^3)

P = density (kg/m^3)

V = velocity (m/s)

This is the main parameter that is important in determining the transmission and reflection at the boundary of two materials having different impedances.

What drill-hole environment is required?

Basically density measurements can be done in any environment, but any change in environment requires a change in calibration parameters. For example, for the same formation, if logging is carried out in a steel-cased hole the gamma rays will be attenuated compared to logging in an open hole. Therefore, steel-cased calibration parameters should be used in a hole with steel casing and open-hole calibration parameters should be used in an open hole.

What do the data look like?

The density of rocks is affected by porosity, water content, and composition. Most of the density variations within igneous and metamorphic rocks are due to variations in mineralogical composition. Rocks with higher percentages of mafic materials (iron- and magnesium-silicate minerals) have higher densities than those with higher percentages of felsic minerals (Ca-, Na-, K-, and Al-silicate minerals). The presence of minerals containing heavy elements such as base metals increases the overall density of the host rock. In sedimentary rocks, density variations may be a result of differing degrees of compaction (indurations) rather than changes in elemental composition. Also, alteration such as silicification reduces the total porosity of a rock and hence there is an associated increase in density. The density log is also useful for locating fractures since open fractures intersected by the borehole often appear as low-density zones on the density log (Wilson et al., 1996).

Density data are used in mapping alteration and identifying rock types by their characteristic signatures. Figure 44 shows lithology, density, and PIMA (portable infrared mineral analyzer) analysis logs from Read Lake, Athabasca Basin. The PIMA analysis effectively defines local-scale alteration zones, and complements alteration mapping as an exploration tool by providing the geochemical composition

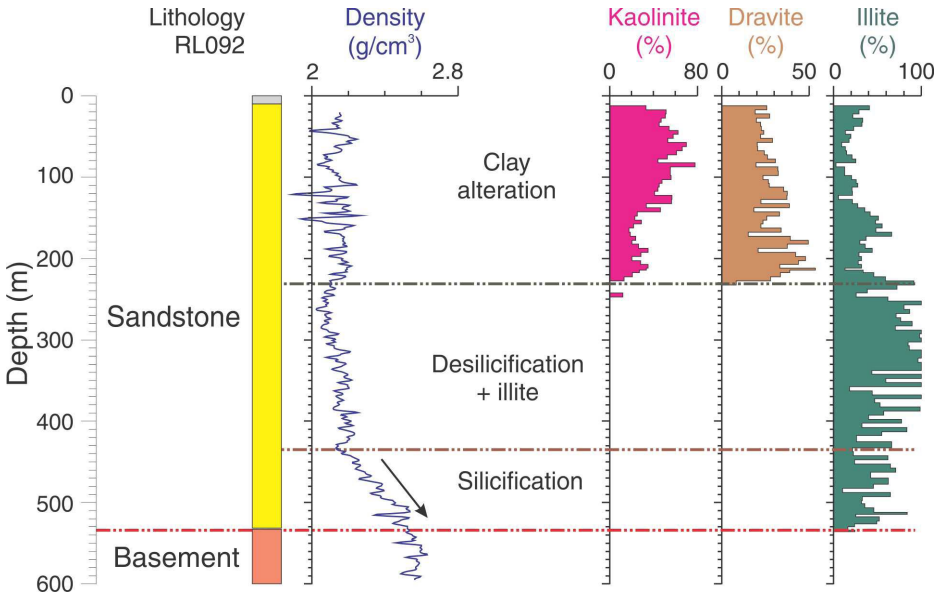

Figure 44. Density log and clay alteration logs (kaolinite, dravite, and illite) from the Read Lake area, McArthur River, Athabasca Basin. All the three clay alteration logs were acquired only in the Athabasca sandstone and show that kaolinite and dravite are virtually zero below 230 m.

of core samples. Notice that silicified zones show an increase (indicated by arrow) in density because of a decrease in porosity.

Density logging can only be done by operators that are trained and licensed to operate, transport, and store active radioactive sources. Once the data are acquired an expert is needed to process the data (i.e. apply all the correction and calibration factors), integrate the data with available geological and geochemical data, and develop an interpretation of these combined results.

Temperature logging

Temperature has many applications in diverse fields. Basically it is quick and easy to use in almost any borehole environment. The temperature probe is really just an extra-large thermometer. It can be used in lithology mapping, where there are environmental concerns in mine planning or development, to track groundwater flow, and to detect radiogenic heat flow (i.e. radiogenic heat production from the concentrations of the radioactive elements).

Figure 45 shows the thermal conductivity of some sulphide minerals, igneous, and sedimentary rocks. The sulphide minerals have the highest thermal conductivity reading and this makes them easy to detect. Sedimentary rocks have the lowest readings. Remember that high conductivity is associated with low-temperature readings.

Why are the temperature data useful?

Mapping lithology

Figure 46 is an example of one lithology log and three temperature-gradient logs (made in the same hole, but at different months and years). Temperature logs are the actual temperatures registered by the probe as it moves down or up the hole. These data are then converted into temperature gradients. Temperature gradients are the change in temperature as a function of depth. Notice the repeatability of the data and how the limestone and shale interbeds have high and low temperature gradients as the probe passes through these narrow beds of different thermal conductivities. In contrast the logs over the more homogeneous limestone area (290–410 m) show less variability.

Figure 47 shows lithology, temperature-gradient, and temperature logs from a massive-sulphide area. Notice the sulphide zone has a very narrow zone of argillite within it. This argillite area can be clearly seen in the spike on the temperature-gradient log.

Mapping groundwater flow

Another example of the use of temperature logs is the mapping of groundwater flow (Fig. 48). Here there is a drastic change in temperature at the water entry zone (indicated by the arrow). There is almost an artesian type of water flow with an upward flow from about 260 m to the top as shown by the almost flat line in the logs. This information would be of significant interest for any mine planning where there will be pumping of water or a need to plug the water-entry zones.

Mapping fracture zones

Figure 49 has data from Shea Creek in the western Athabasca Basin area. This is an example of how useful it can be to acquire temperature data immediately after drilling. Temperature anomalies due to fracture zones are apparent at this time. Here the warm fluid used during drilling has been forced into areas where there are fractures and thus higher permeability. When the drill is removed and the

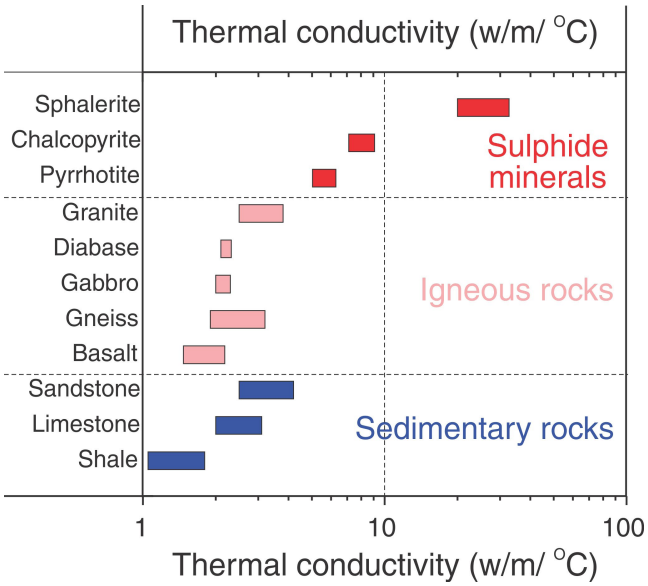

Figure 45. Thermal conductivity of some common rocks and sulphide minerals. Notice that among the sedimentary rocks, the sandstone has the highest thermal conductivity.

temperature log acquired immediately, the rock-wall areas that were more permeable will have absorbed some of the warm drill fluid and will show clearly in the logs.

Identifying radiogenic heat

The last example of temperature data indicates an area of radiogenic heat generation (Fig. 50). What could be causing that? High-grade uranium generates heat and this fact caused a few surprises for the mining engineers when the McArthur River mine was opening. To mine ore at this site it is necessary to freeze the rock so it can be removed easily. Calculations were done to determine the amount of energy necessary to do this freezing; however, the amount of radiogenic heat generated by the very high-grade ore at this site was not factored into the original calculations! Further information about temperature logging can be found in Mwenifumbo (1993).

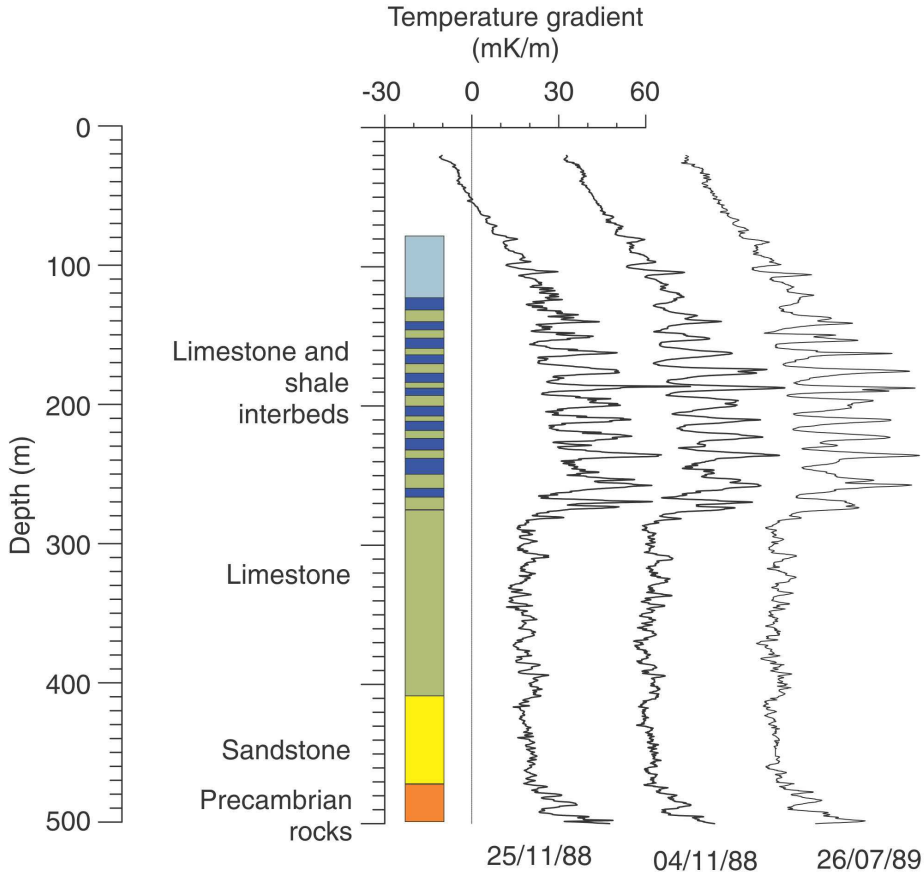

Figure 46. Limestone, shale, and sandstone have different thermal conductivities and are therefore easily identified on temperature-gradient logs. Three temperature logs are displayed in this figure; the first two were acquired approximately two weeks apart and the last one was acquired about eight months later. All show identical signatures.

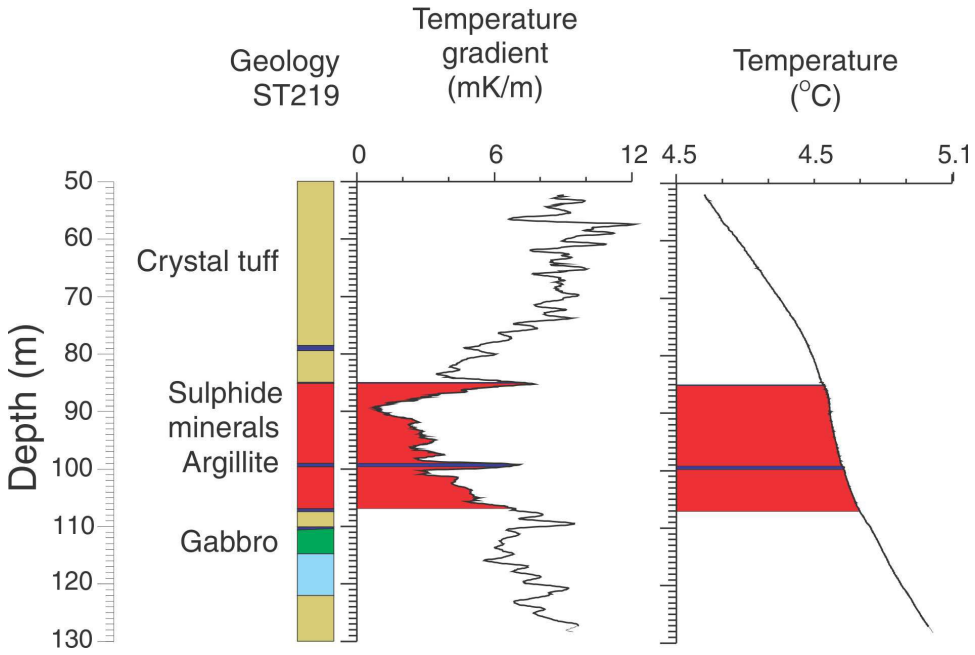

Figure 47. Lithology, temperature gradient, and temperature logs acquired through a massive-sulphide deposit in New Brunswick.

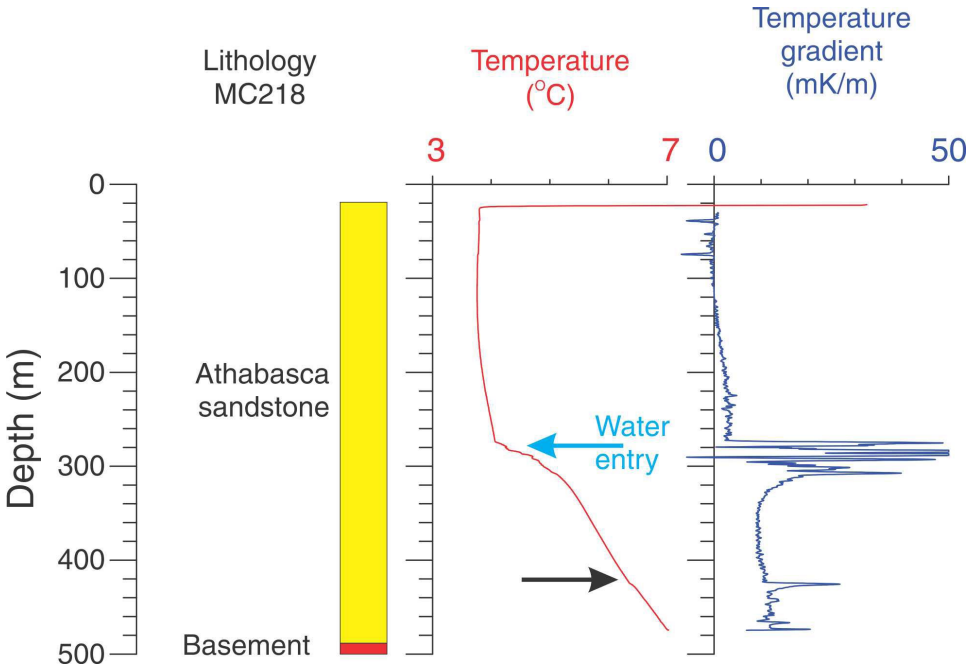

Figure 48. Temperature- and derived-temperature–gradient logs acquired at McArthur River deposit, Athabasca Basin, Saskatchewan.

Less common methods and exotic

There are five borehole geophysical methods that are not commonly used in uranium exploration: however, they are being briefly covered in this section. These include borehole imaging, neutron porosity, X-ray florescence (XRF), prompt fission neutrons (PFN), and mise à la masse.

Borehole-imaging method

Electrical, acoustic, and optical televiewers can be presented as a 3-D image of the borehole wall that looks like the drill core. A computer-generated 'synthetic drillcore' will look very much like the real thing. For a view of the product from televiewers, visit GEOVision's web site at (http://www.geovision.com) or the Robertson Geologging Ltd. site at (http://www.geologging.com).

Neutron-porosity method

The neutron-porosity method uses a chemical neutron source to measure the porosities of formations. It is similar to the gamma-ray method, but the detector measures neutrons instead of gamma rays. Hydrogen has the largest effect in slowing down and capturing neutrons. Pore fluids are generally rich in hydrogen, so a measure of porosity can be made; however, the type of rock formation and fluid also has an effect. The log must be calibrated correctly to reflect this. Hydrogen occurs in clay minerals and hydrated minerals as well as pore fluids. Gas has a low hydrogen density, so that gas zones have a very low apparent porosity. Neutron-porosity logs aid in mapping alteration (i.e. silicification, chloritization, hydrous minerals). Figure 51 shows lithology, resistivity, and porosity logs.

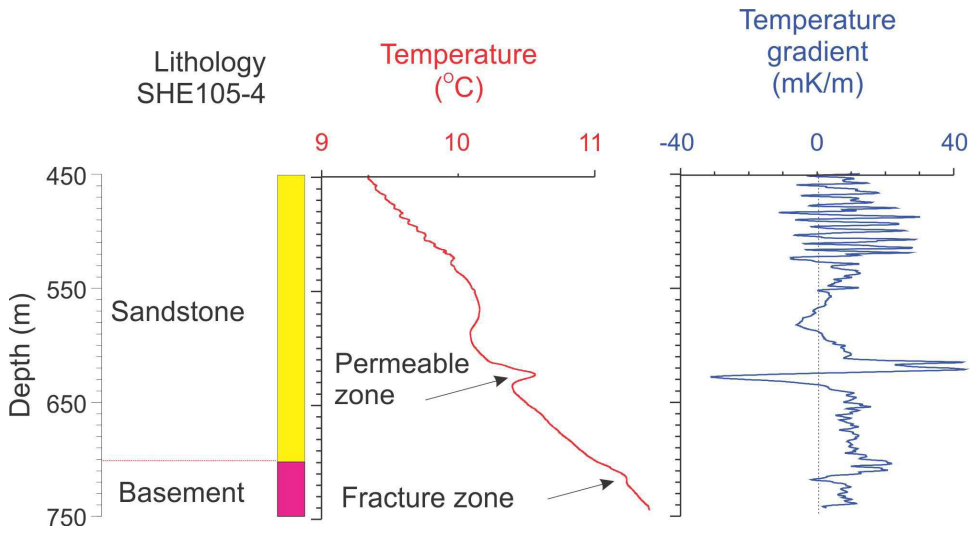

Figure 49. Example of temperature- and temperature-gradient–log responses in permeable and fractured rock, where drilling fluids that are warmer than the formation waters have infiltrated the formation and created high-temperature anomalies. These temperature anomalies decay over time as the borehole-fluid temperatures reach the formation-fluid temperatures.

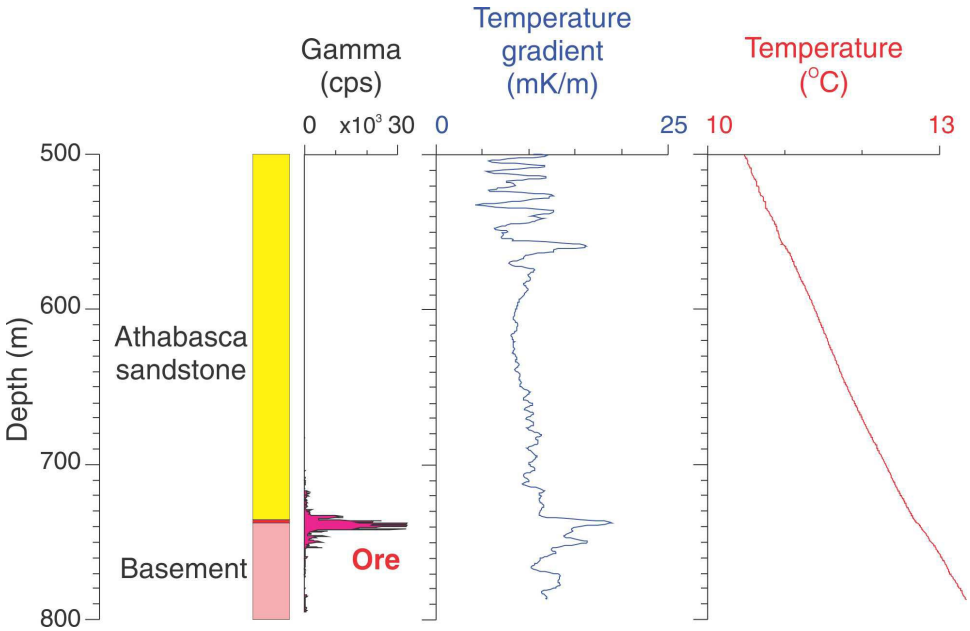

Figure 50. Gamma-ray log showing the location of uranium ore zone. Temperature logs indicate an anomalous temperature gradient response around the uranium ore zone suggesting that significant amounts of heat are generated from the uranium mineralization to change the normal temperature gradient (geothermal gradient).

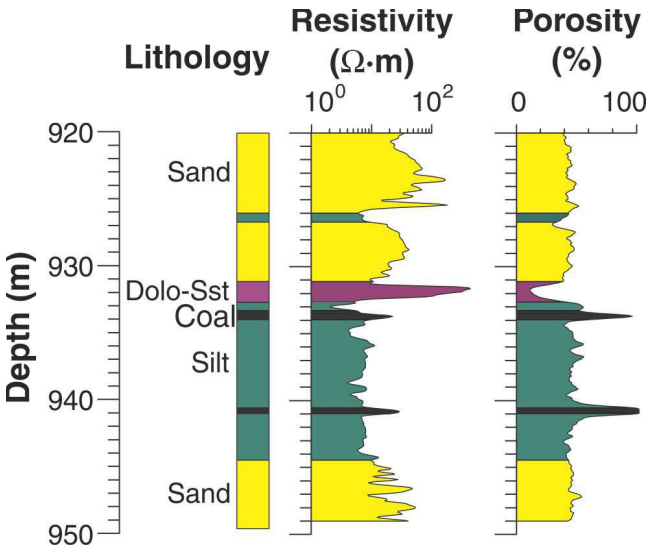

Figure 51. Resistivity and porosity logs acquired through a slit-sand formation with coal and dolomitized sandstone (Dolo-Sst).

In the dolomite-sandstone area there is high resistivity and low porosity due to silicification. In this case, resistivity is a function of porosity; however, the two coal seams exhibit relatively high resistivity and high porosity. In this case, the high porosity readings are not due to an increase in pore spaces, but due to the presence of hydrogen in the coal.

X-ray fluorescence method

In uranium exploration, X-ray fluorescence (XRF) can provide a solution to the 'disequilibrium problem' by measuring uranium directly (and not indirectly from daughter products). If the uranium has migrated to another location, the gamma-ray log cannot be relied upon to indicate the correct grade. The grade calculation made from the gamma-ray log can be either optimistic or pessimistic. Uranium may have moved into an area of low gamma rays thus increasing the grade or out of an area of high gamma rays thus decreasing the grade. When this occurs, the orebody is said to be in disequilibrium (*see* 'Gamma-ray and spectral gamma-ray logging').

If a uranium ore deposit is in a hard-rock environment, there is good agreement between lab analyses of the amount of uranium present in core samples and natural gamma-ray logs. Over time the decay products measured by gamma-ray logging will be directly proportional to the uranium in the formation provided that geological processes (i.e. water flow or other events) have not caused the uranium to be separated from the gamma-ray emitters being measured.

In a sandstone-hosted uranium deposit, however, disequilibrium is likely to occur with an accompanying water flow. Here, movement of uranium out of the deposit results in an overestimation of the amount of uranium present. What is occurring is that the breakdown of uranium produces daughter products and radon gas. These are radioactive and create inflated readings that do not reflect the actual quantity of uranium ore present, since typical gamma-ray logging tools measure radioactive decay products rather than the ^{235}U of interest.

In a roll-front type of deposit, a shortage of daughter products relative to uranium (because this type of deposit is usually young in geological terms) will cause an underestimation of uranium content based on radiometric methods. Therefore, disequilibrium can vary from place to place.

Prompt-fission neutron logging tool

This system provides another way of getting around the disequilibrium problem discussed above. The prompt-fission neutron (PFN) logging tool overcomes this problem by directly measuring the uranium in the formation using a pulsed neutron source that generates neutrons that cause fission in the uranium in the formation. The neutrons returning to the system from the formation are counted in detector channels to provide a measure of uranium. As with some of the other logging systems, the PFN tool must be calibrated at a calibration facility.

Mise à la masse (MALM) technique

The mise à la masse technique is another electrical resistivity method that can be used to outline electrically conductive zones (Mwenifumbo, 1997). Most orebodies are structurally complex, highly deformed, and faulted. Therefore, the determination of the orebody geometry, even after expensive definition drilling, is often difficult. With this method, measurements can be done on the surface or in boreholes to delineate the orebody and to determine if two orebodies are connected. In the Athabasca Basin uranium deposits, graphitic structures and fault zones are closely related to uranium mineralization. These structures are electrically more conductive than the unfractured sandstone or basement rocks.

The mise à la masse technique would provide variable information on the orientation of graphitic structures and the relationship between different fracture sets and hence aid in the interpretation of relative movements between these structures (Fig. 52).

Figure 53 shows a typical mise à la masse system. This equipment can be set up using two kinds of electrode arrays (i.e. potential and potential gradient). With the normal array, there is a transmitter that has two electrodes. The first is a fixed-current electrode that is placed in a conductive zone and the second is a return-current electrode that is placed on the surface, effectively at electrical infinity. The second part of the system is seen on the right side of the figure. In the potential array, there is a fixed reference potential electrode at infinity and the other electrode moves from one

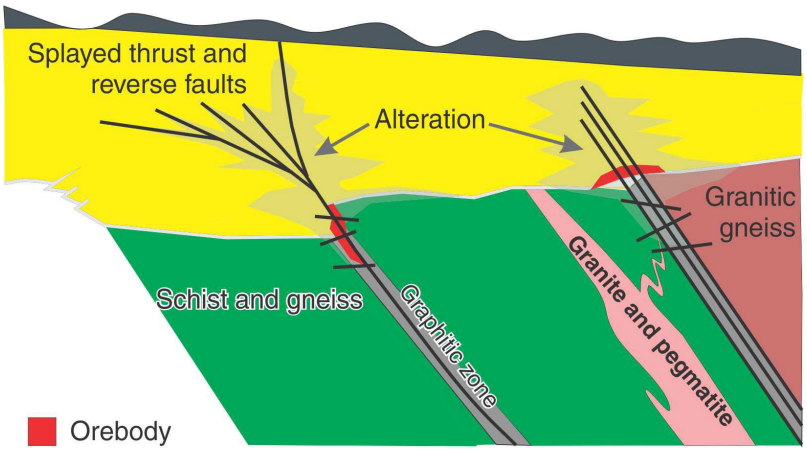

Figure 52. Geological model of the unconformity-related uranium deposit in the Athabasca Basin (Jefferson et al., 2007).

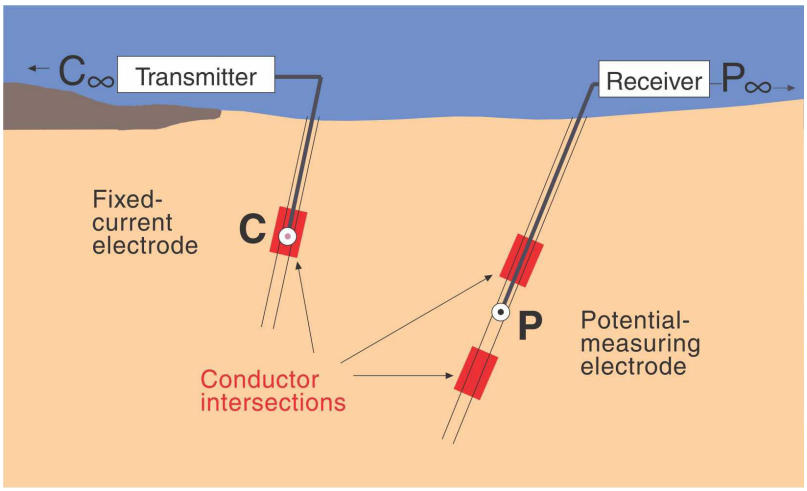

Figure 53. Electrode array set-up in downhole mise à la masse measurements. This set-up is usually used in sorting out the relationship between conductor intersections.

observation point to another. In the potential-gradient array, the fixed reference current electrode is still set at infinity, but the probe contains two potential electrodes set at a fixed distance apart with the difference being calculated in the measurements made at each of these two electrodes. These two electrodes are then moved in tandem and the orebody is mapped in this manner.

Figure 54 shows two drillholes: hole #1 intersects one conductive zone in the upper part of the hole and hole #2 intersects two conductive zones. The resistivity log shows that both the structures in hole #2 are very conductive. It would be useful to know if the conductive zone in hole #1 is connected to either of the zones in hole #2. When a current is passed through the conductive zone in hole #1, the MALM P (mise à la masse potential) log in hole #2 shows a corresponding peak at the location of the upper conductive zone. Therefore, the conclusion is that the conductive zone in hole #1 is connected to it. There is no connection between the zone in hole #1 and the lower zone in hole #2.

The scenario presented in Figure 54 is generally what would be expected; however, Figure 55 provides another example that appears to be similar geologically, but the interpretation of the conductivity structure geometry is different. The mise à la masse potential measurements in hole #2 when the conductive structure in hole #1 is energized, shows a potential high in the lower conductive zone, indicating that the conductive zone in hole#1 is connected to the lower zone in hole #2.

GAMMA-RAY PROBE CALIBRATION SITES

Introduction

In uranium exploration, the uranium grades are determined from gamma-ray logs. Gamma-ray probes have to be calibrated to provide accurate grades. Also because the probes are prone to drift due to field handling and aging, they have to be frequently recalibrated. The logging systems have to be calibrated at a standard calibration site prior to and after each field-logging season to ensure consistency of grade estimation.

In Canada there are two main calibration facilities: Saskatchewan Research Centre (SRC) pits in Saskatoon, Saskatchewan; and the Natural Resources Canada Bells Corners

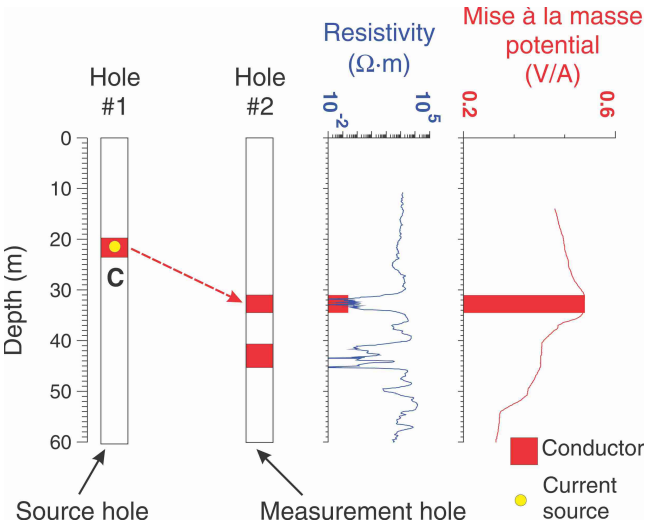

Figure 54. Mise à la masse potential measurements in hole #2 with the current source located at C in hole #1. Also shown in the figure is the normal-array resistivity log, indicating two conductive zones in hole #2.

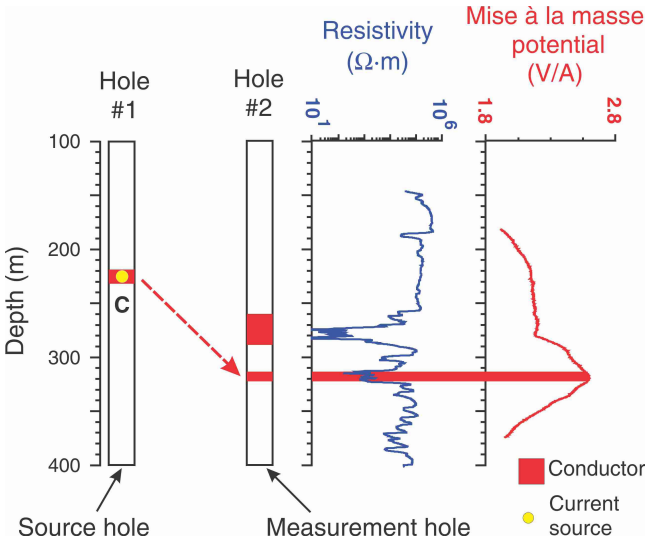

Figure 55. Mise à la masse potential measurements in hole #2 with the current source located at C in hole #1. Also shown in the figure is the normal-array resistivity log, indicating two conductive zones in hole #2.

facilities in Ottawa, Ontario. In the United States, calibration facilities are administered by the U.S. Department of Energy (DOE) and their sites are located at the Grand Junction Regional Airport in Grand Junction, Colorado; Grants, New Mexico; Casper, Wyoming; and George West, Texas. An additional calibration facility is located at the DOE Hanford site near Richland, Washington, and is managed by the DOE Office of Environmental Management.

These calibration facilities are used by instrument manufacturers and field-logging crews to calibrate gamma-ray logging systems. All these sites have models constructed of concrete with known, uniform concentrations of naturally occurring potassium, uranium, and/or thorium. The SRC pits have uranium models only for calibrating total-count gamma-ray logging systems. The Bells Corners and Grand Junction facilities can be used to calibrate either total-count or spectral gamma-ray logging systems.

Saskatchewan Research Centre calibration facility

The Saskatchewan Research Centre test pits are located in Saskatoon. Clients can access this facility on a fee-for-service basis. There are four models at the site (Fig. 56).

Pits 1, 2, and 3 have 'infinite thickness' ore zones (i.e. >1 m), whereas pit 4 is a 'thin zone' (21 cm thick). Pits 2 and 3 are homogeneous and a stationary log acquired in the centre of the ore zone is adequate for determining the calibration factors. The ore zone in pit 1 is not homogeneous. It is recommended that an average count rate (I) be determined in the 'plateau' region from a slow continuous log through the ore zone. The k-factor is then determined from the relation G = kI, where G = grade and I = average count rate determined from the average count rate in the middle of the ore zone.

For the thin pit 4 ore zone, the standard procedure of determining the count rate in the centre of the ore zone does not work. Here a slow continuous log must be acquired and the area under the curve is used to establish the k-factor. Table 6 gives the concentrations of uranium (G) and the thickness of the ore zone (T) in these models. Determine the area (A) under the anomaly and then compute the k-factor where GT = kA. Construction of an additional model(s) at the site with a higher concentration of uranium has been proposed.

Bells Corners borehole calibration facility

The Bells Corners calibration facility is located in the west end of Ottawa at the CANMET complex. It consists of two sites and is operated on a fee-for-service basis. Site 1 has six deep holes ranging in depth from 120 m to 300 m that intersect various Paleozoic and Precambrian formations and structures with varied physical-rock properties. The six deep holes are available to calibrate instruments for standard borehole geophysical measurements of porosity, resistivity, induced potential, conductivity, sonic velocities, density, total-count gamma ray, magnetic susceptibility, and temperature. Detailed information on the geological interpretation and geophysical logging results from the six deep boreholes may be found in Bernius (1996).

The second site consists of nine calibration columns that are concrete-encased boreholes of potassium (K), uranium (U), and thorium (Th); ten concrete K, U, and Th pads for calibrating portable gamma-ray spectrometers;

five density-calibration rock blocks, and a concrete hole-size model. The nine columns consist of three K, three U, and three Th models with varying concentrations. Table 7 gives the concentration of each of these model columns. A schematic figure of one of the models (Fig. 57) shows the barren zones and ore zone and a typical gamma-ray response through the ore zone. Notice that within each model there are three holes, each with a different diameter (i.e. AQ = 48 mm, BQ = 60 mm, and NQ = 75.7 mm). The rock blocks and borehole size model are used for calibrating density probes.

Additional details on this calibration site may be found in a report by Mwenifumbo et al. (2005).

Grand Junction models

The gamma-ray pits at Grand Junction are large concrete cylinders with 4.5 inch diameter test holes with uniform concentrations of potassium, uranium, and thorium. These facilities can be used to calibrate total-count or spectral gamma-ray logging systems. If logging measurements are to be carried out in water-filled boreholes, then a water correction must be made to the logs based on the measurements in the water-factor model (KUT WTR). Table 8 gives the grades assigned to these models.

CASE STUDIES

This section presents five scenarios highlighting situations or problems that commonly occur during uranium exploration. As each scenario is presented it is useful to think about the geological environment, drillhole environment, and deposit type as this information dictates the geophysical techniques that are appropriate.

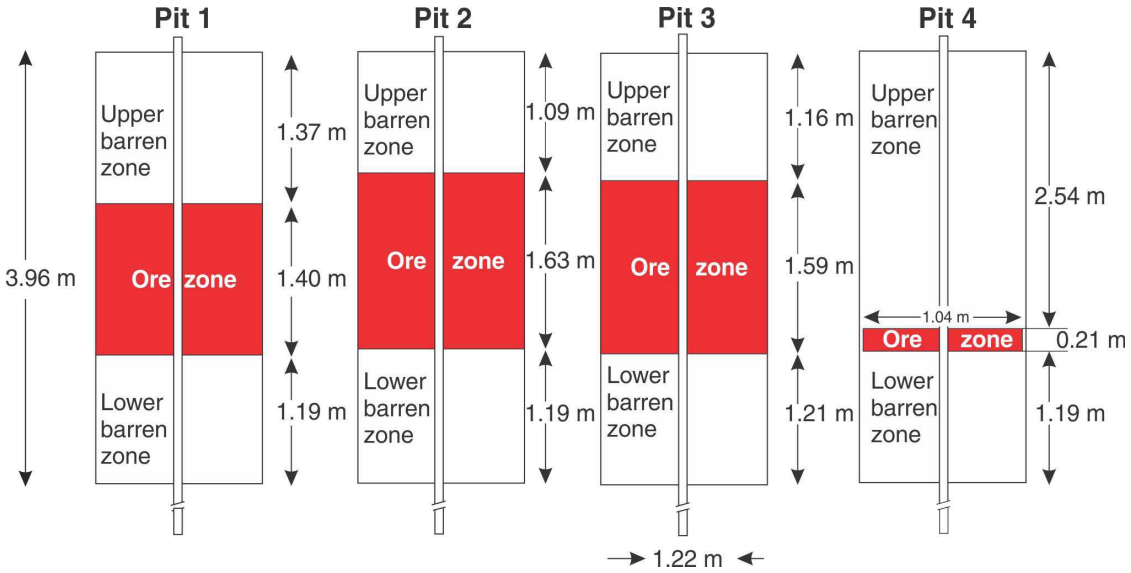

Figure 56. Four calibration pits at the SRC facilities in Saskatoon, Saskatchewan, showing the thickness of the U ore zones (K.A. Pflug and C.J. Mwenifumbo, unpub. report, 2006).

Table 6. Grades and thickness of SRC pits (Quirt and Elash, 2006).

Uranium model pit #	Grade U (%)	Thickness (m)
1	0.06	1.40
2	0.30	1.63
3	1.35	1.60
4	4.15	0.21

Table 7. Concentrations of potassium, uranium, and thorium in each of the models (Mwenifumbo et al., 2005).

Model #	K (%)	U (ppm)	Th (ppm)
BK-1-OT	0.80 ± 0.21	0.37 ± 0.15	0.44 ± 0.40
BK-2-OT	1.25 ± 0.12	0.27 ± 0.15	0.86 ± 0.38
BK-3-OT	3.28 ± 0.20	0.28 ± 0.25	1.24 ± 0.30
BU-4-OT	0.31 ± 0.07	15.7 ± 11.3	0.79 ± 0.40
BU-5-OT	0.25 ± 0.03	107.6 ± 27.4	0.75 ± 0.23
BU-6-OT	0.25 ± 0.03	997.9 ± 129.7	0.75 ± 0.23
BT-7-OT	0.16 ± 0.03	1.13 ± 0.19	10.97 ± 0.51
BT-8-OT	0.23 ± 0.07	3.15 ± 0.55	50.20 ± 5.00
BT-9-OT	0.30 ± 0.14	27.2 ± 2.3	503.5 ± 17.20

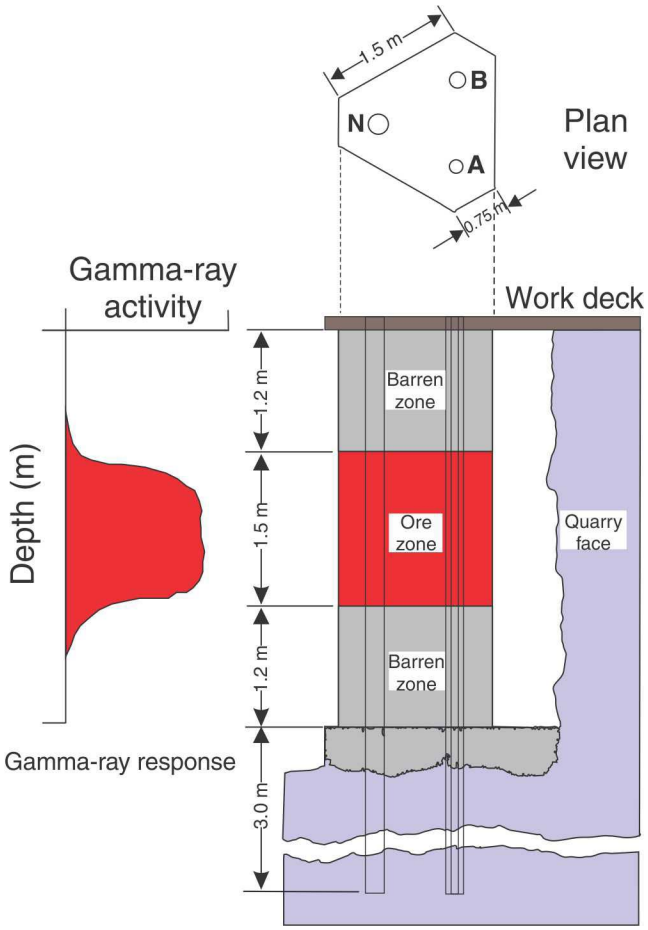

Figure 57. Schematic of the Bells Corners model boreholes for calibrating gamma-ray probes.

Unconformity-related deposit

Figure 58a shows a schematic from the Cigar Lake deposit in the Athabasca Basin. There are two sandstone-hosted deposits and one large unconformity-related deposit. Extensive silica and clay alteration is associated with this deposit type.

In the schematic from the McArthur River deposit (Fig. 58b), a low-grade and a high-grade basement-hosted deposit are shown. In addition, there is an unconformity-related deposit on the fault zone. What geophysical methods should be used in these deposit types?

Total-count and spectral gamma-ray logging

Natural gamma-ray logging will assist with mapping the sandstone stratigraphy and provide some in situ uranium grade determinations. Figure 59 shows total-count and spectral gamma-ray logs from the McArthur River deposit.

The total-count gamma-ray log shows two major anomalously high gamma-ray activity zones in the MFb stratigraphic horizon. The spectral logs reveal that the upper anomaly on the total-count log is due to the presence of thorium from the mineral crandallite (Mwenifumbo and Bernius, 2007), whereas the lower anomalous zone is due to a mixture of uranium and thorium. This example illustrates the importance of spectral gamma-ray logging measurements for accurate in situ uranium grade determinations. Note the high potassium counts in the pelite and semipelite in the basement rocks as these will affect uranium grade determinations.

Table 8. Grades of the potassium, uranium, thorium, and the KUT water-correction models (Stromswold and Wilson, 1981).

Model	K (%)	U (ppm)	Th (ppm)
Potassium	6.76 ± 0.18	2.7 ± 0.3	2.4 ± 0.6
Uranium	0.84 ± 0.24	498.3 ± 12.1	5.6 ± 1.3
Thorium	1.44 ± 0.08	28.3 ± 1.0	505.5 ± 12.1
KUT WTR	4.90 ± 0.29	321.0 ± 19.0	219.4 ± 9.2

Resistivity and IP

The resistivity and IP methods facilitate mapping of alteration and conductive structures associated with uranium mineralization. In Figure 60, the upper portion of the hole consists of silicified sandstone units that have high resistivities and can be distinguished from the dissolved and fractured clay units just below that have low resistivities. In the basement rocks, the IP log identifies the conductive shear and fractured graphitic gneiss and basement faults.

Density and seismic velocity

These methods give information on the physical properties of the sandstone and basement structures as well as the unconformity. The density logs would show that in the upper portion of the hole the silicified sandstone units have high density, whereas the dissolved, fractured clay alteration zone just below has low density. The basement rocks have higher densities than the sandstone units (except for the quartzite units, which are basically sandstone). Velocity logs would show high velocity for the silicified sandstone units and lower velocity in the clay area. In the basement rocks, the unaltered rock would have high velocity, whereas the graphic gneiss areas would have lower velocity.

Data integration

Figure 61 of the Read Lake deposit shows lithology, total-count gamma-ray, resistivity, density, velocity, and drillcore sample logs. Like a jigsaw puzzle, each piece is interesting on its own, but one must put them all together for the whole picture to emerge. From 100–150 m is silicified sandstone where resistivity, density, and velocity are high. In the unconformity zone, resistivity, density, and velocity increase (as a function of silicification) toward the basement.

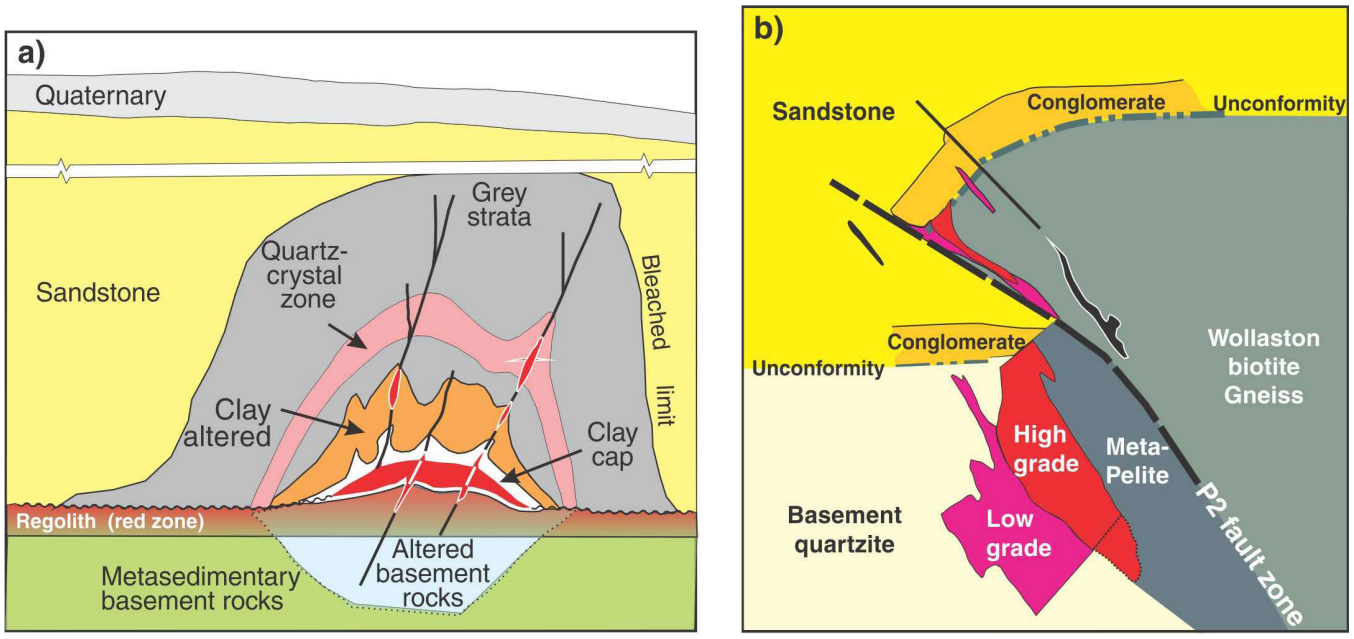

Figure 58. a) A schematic of an unconformity-related sandstone deposit in the Athabasca Basin (*modified from* Jefferson et al., 2007); **b)** section of basement-hosted and unconformity- and/or fault-related deposit from the McArthur River deposit (modified section supplied by mine geologists during the EXTECH IV project (Staff of McArthur River mine, pers. comm., 1999)).

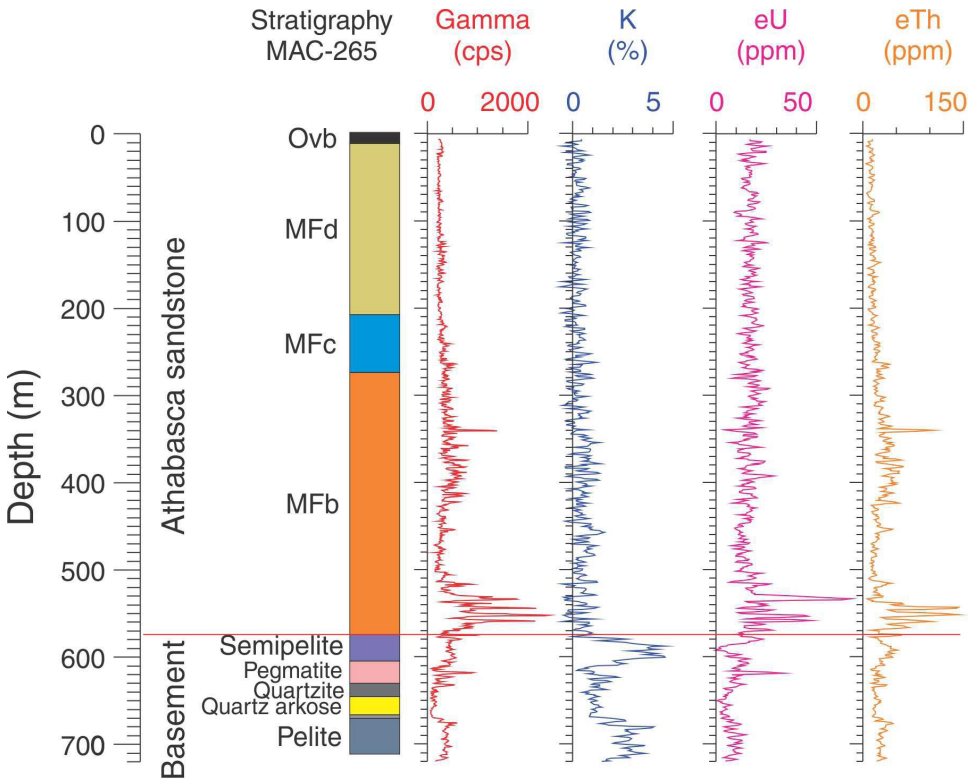

Figure 59. Formation, total-count gamma-ray, and spectral gamma-ray (K, U, Th) logs from the McArthur River deposit. The Athabasca sandstone units consist of the Manitou Falls Formation (Dunlop Member (MFd), Collins Member (MFc), and Bird Member (MFb); Ovb = overburden.

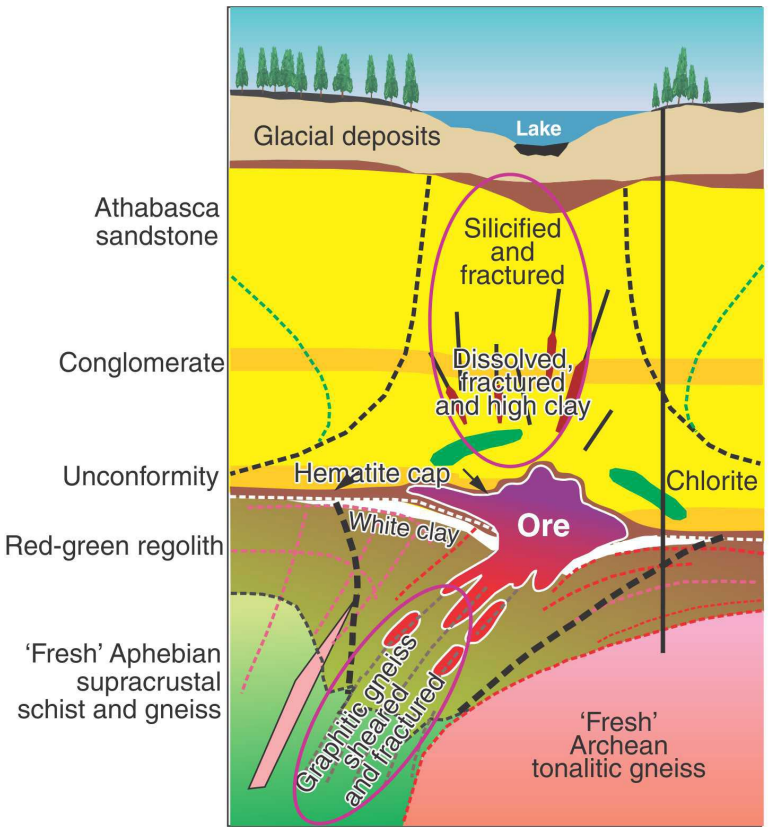

Figure 60. Ore-deposit model showing the alteration and structures associated with uranium mineralization (*modified from* Jefferson et al., 2007). Structures and alteration features that significantly alter the electrical properties of the Athabasca sandstone include silicification, clay alteration, and fractures. In the basement rocks shear, fracture, and graphic zones have very distinct electrical properties compared to the fresh basement rocks.

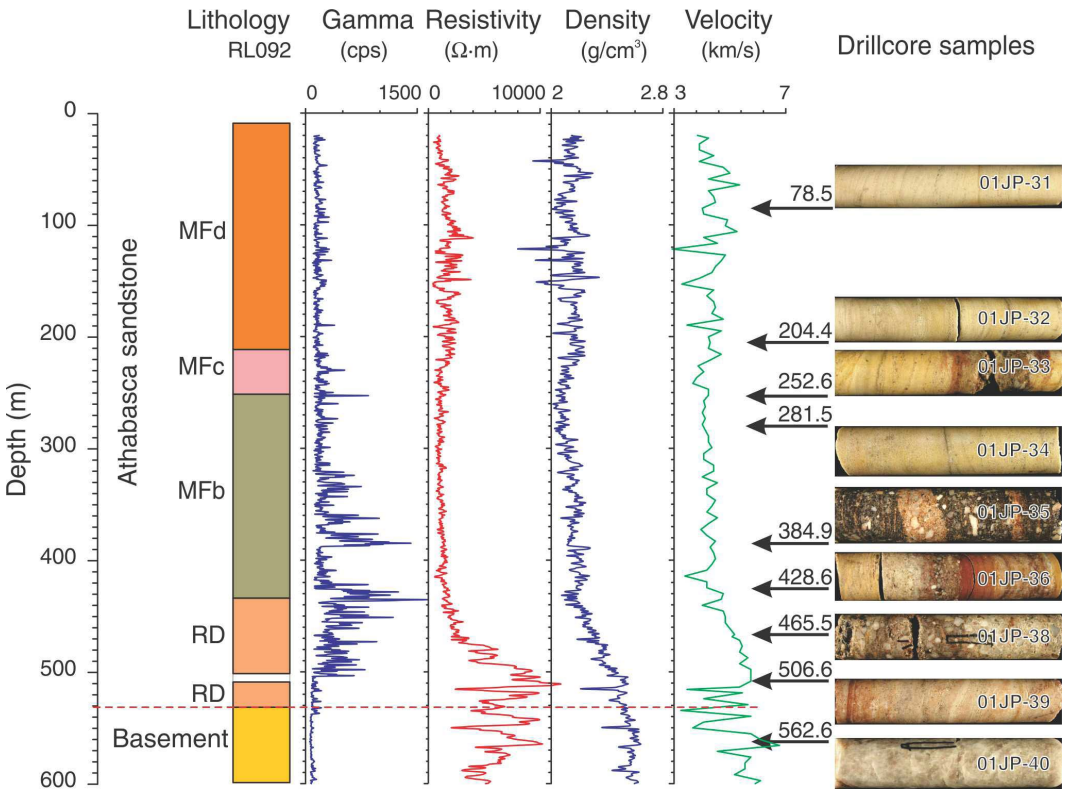

Figure 61. Gamma, resistivity, density, and velocity logs acquired in a McArthur River deposit. Also shown to the right of the figure are some photographs of selected drill-core samples. The high resistivities, densities, and velocities in MFd (100–225 m) are due to silicification. Photographs by J. Mwenifumbo. Lithology: Manitou Falls Formation (Dunlop Member (MFd), Collins Member (MFc) and Bird Member (MFb)); RD = Read Fromation

In the basement, resistivity and velocity variations are due to fracturing. It should be noted that the basement rocks are quartzite and so their readings are not too different from the sandstone units.

Athabasca Basin problems

The Athabasca Basin has some unique exploration problems. These include anomalously high potassium and thorium concentrations and extremely high uranium grades in some areas. Spectral gamma-ray logging can help to sort out the first problem as it gives separate logs for uranium, thorium, and potassium. High-grade uranium presents several challenges. First, as calibration facilities do not have models with high uranium grades, the completely accurate calibration of logging systems for use in the Athabasca Basin high-grade uranium areas is not possible at the present time. Second, in a very efficient gamma-ray detector (e.g. the BGO) the actual count rates in the ore zone may get reduced as the detector is 'blinded' by an overload. One possible solution that is commonly adapted is to use a poor detector in terms of efficiency (e.g. Geiger Müller). Density logging is not possible in high-grade uranium situations as negative densities are recorded because the natural gamma rays from the uranium overwhelm the gamma rays coming from the source used in the logging system; however, if spectral gamma-gamma logs are available, the ratio of the high-energy window (HEW) to the low-energy window (LEW) readings will give the spectral gamma-gamma ratio (SGG). This ratio will provide the relative uranium grades (Fig. 62). For further discussion of spectral gamma-gamma ratio in uranium exploration *see* Killeen (1997).

Sandstone roll-front deposit

In sandstone deposits, natural gamma-ray logging can provide information on stratigraphy and in situ uranium grades. The four holes shown in Figure 63 intersect various sections along the roll-front deposit. The gamma-ray log would show elevated count rate in the confining mudstone and very low count rates in the clean, unaltered sandstone (hole 4). The count rates in the altered hematite-limonite section near hole 1 would be low and then increase laterally as one approaches the ore zone. Very high count rates would be observed in the ore zone (hole 2).

Resistivity and IP measurements can aid in pyrite detection and pinpoint the hematite and limonite areas (Fig. 63). Hole 1 on the left passes through a hematite-limonite zone that would show up as a low-resistivity zone with relatively higher IP compared to the unaltered sandstone. Hole 3 on the right passes through unaltered sandstone (low IP, high resistivity), pyrite (high IP, low resistivity), and then through sandstone again. The mudstone units generally have higher conductivity than the sandstone. Figure 64 shows how the conductivity can be used to improve the stratigraphy of a roll-front deposit. In several cases the holes in these deposits are percussion drilled and hence the delineation of the intersected geology is very poor.

Quartz-pebble conglomerate deposit

The Elliott Lake deposit is of the quartz-pebble conglomerate type. This area saw the operation of 14 mines, with the last one closing in the mid 1990s due to decreases in demand and the lower costs associated with producing uranium from

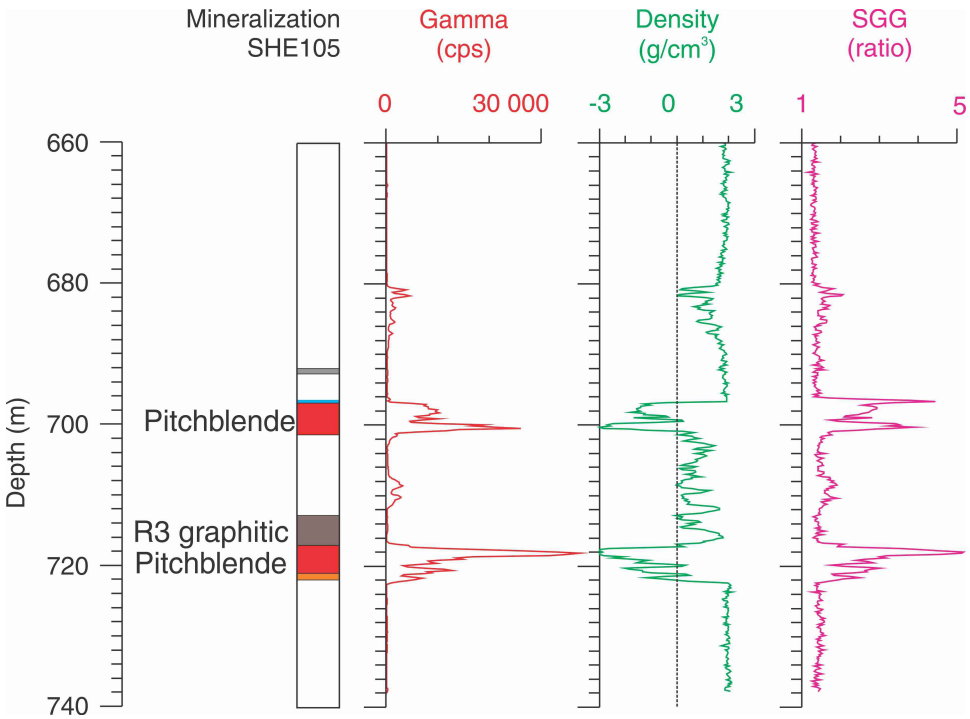

Figure 62. Hole in the Shea Creek deposit drilled through very high concentrations of uranium. The standard gamma-gamma density logging for acquiring in situ density measurements does not work in this case (negative densities are observed). The spectral gamma-gamma log (SGG) clearly outlines the uranium ore as a heavy element.

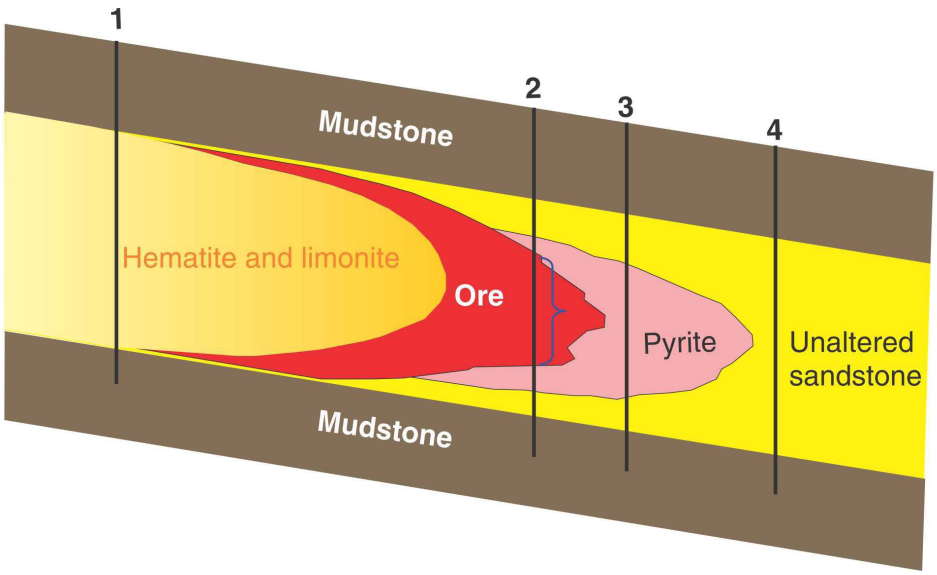

Figure 63. Schematic of a roll-front sandstone deposit (*after* Devoto, 1978).

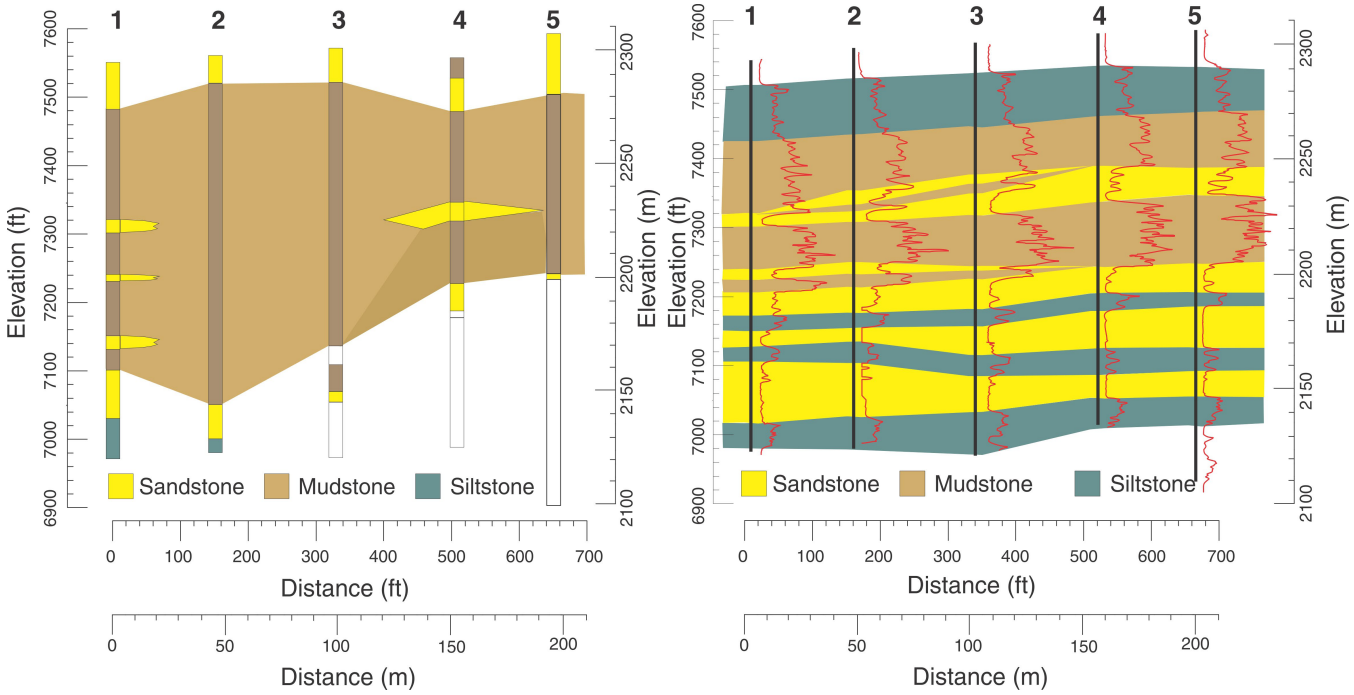

Figure 64. Section of holes drilled through a roll-front deposit. The figure on the left shows a geological section constructed from drill-chip sample observation and the section on the right is based on borehole EM conductivity log data. There is very distinct signature between the mudstone, siltstone, and sandstone. The highest conductivities are observed in the mudstone, followed by the siltstone, and very low conductivity is observed in the sandstone.

higher grade deposits (e.g. Athabasca Basin). In this area, gamma-ray spectrometry was used to map stratigraphy and to allow for accurate uranium grade determination in zones where there were high amounts of thorium. Resistivity and IP methods could be used to detect pyrite (high IP, low resistivity) and to distinguish between quartzite (high resistivity) and argillite (high IP, low resistivity).

Breccia complex deposit

The Olympic Dam deposit in South Australia is an iron-ore-copper-gold (IOCG) deposit that contains significant quantities of uranium. Olympic Dam is the world's largest resource of low-grade uranium. In this area, hematite-rich breccia units are dense and electrically conductive compared to the host rocks. Electromagnetic (EM) logs can detect sulphide minerals and hematite. Induced polarization (IP) and resistivity logs facilitate discrimination between different sulphide minerals (lead and zinc versus copper). The lead-zinc-sulphide minerals are less conductive compared to copper-sulphide minerals.

Pegmatite-intrusive deposit

Bancroft, Ontario is an area where four uranium mines operated between 1956 and 1982. In this pegmatite-intrusive deposit, uraninite and other uranium-thorium minerals occur in pegmatite units, within sedimentary and igneous rocks. Hematite is a characteristic alteration product. In this type of deposit where high levels of thorium are a problem, the spectral gamma-ray logs can identify the presence and concentration of uranium, thorium, and potassium. In Figure 65 zones with high gamma-ray activity identified on the total-count gamma-ray log (TC) are not all due to the presence of uranium. Zone 1 in the pegmatite is all uranium, whereas zone 2 has both uranium and thorium present and zone 3 is mostly thorium, with relatively small amounts of uranium and potassium.

A FINAL WORD

Why use borehole geophysics?

In uranium exploration, some still talk about borehole geophysics as ‘the black arts’ or ‘the dark side’ of exploration work. These ideas have really arisen from the inability of the borehole geophysics community to clearly communicate exactly what they do, what they can contribute, and what cost savings their work can generate.

Exploration beneath the surface of the Earth fits very well into the medical model. Initially there are observations of the body’s surface by the medical practitioner. In parallel to this are field observations by the geologist. Then, if something interesting is found, a doctor might order a biopsy. This, of course, is similar to the analysis of rock or drill-core samples. The next step in the medical model might be to order a group of more noninvasive tests such as X-rays, MRIs, PET scans, scopes, etc. In mineral exploration, here is where the borehole geophysicist joins the party. It is much cheaper and faster to get borehole measurements that let you see what is happening beneath the surface from the one or two holes already drilled, than to keep drilling lots of holes.

Aside from the time and money savings gained from logging costs versus drilling costs, borehole data can also give information on the uranium distribution and grade in a deposit, footprint uranium deposits and their host rocks, and provide in situ rock-property information to enhance the interpretation of airborne or surface geophysical surveys.

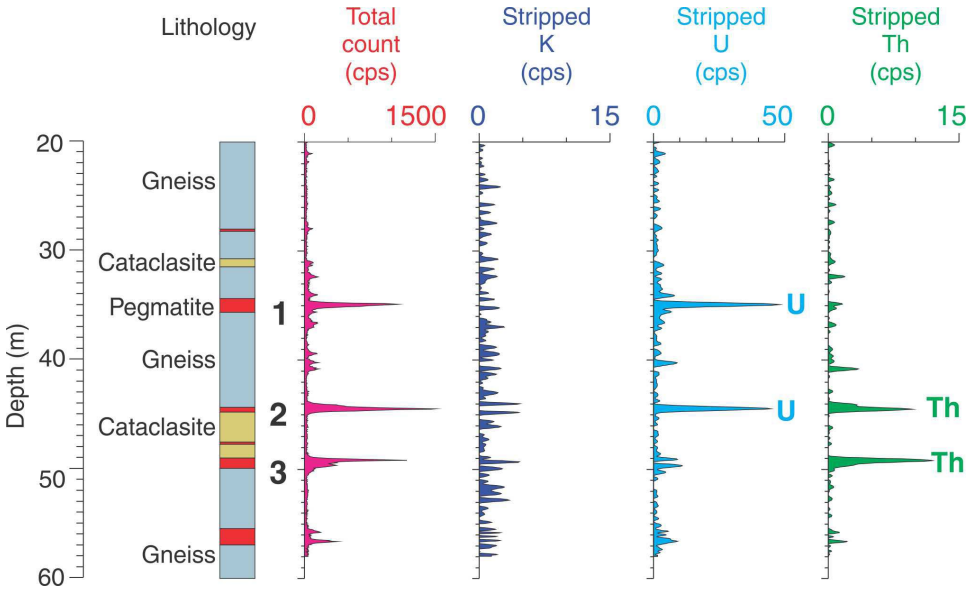

Figure 65. Total-count and spectral gamma-ray logs acquired in a pegmatite-intrusive deposit in the Bancroft, Ontario area.

Cautionary notes

To get the most out of borehole geophysics measurements it is necessary to:

- Plan ahead before drilling as borehole environment affects the methods that can be used.
- Ensure the logging system is calibrated before and after fieldwork (if required by the type of system).
- Use trained technicians to collect the data and produce detailed field sheets.
- Use a trained borehole geophysicist to process, interpret, and integrate these data with the airborne, geochemical, and surface data.

ACKNOWLEDGMENTS

This is a condensed version of the geophysical content of a short course presented in 2008 at the Saskatchewan Open House. The authors wish to thank C. Jefferson (Geological Survey of Canada) for critically reviewing this paper and for his constructive suggestions. The authors also wish to thank the Saskatchewan Research Council, Saskatchewan Geological Survey, AREVA Resources Canada, and Cameco Corporation for sponsoring and/or facilitating the short course.

The authors wish to acknowledge the presenters of the Saskatchewan 2008 Uranium Short Courses: J. Mwenifumbo (GSC), C. Jefferson (GSC), B. Schreiner (SRC), S. Bosman (SGS), C. Card (SGS), S. Creighton (SRC), and L. Mwenifumbo (GSC).

This technical note is a product of Secure Canadian Energy Supply Program.

REFERENCES

Bernius, G.R., 1996. Borehole geophysical logs from the GSC Borehole Geophysics Test Site at Bell's Corners, Nepean, Ontario; Geological Survey of Canada, Open File 3157, 38 p. doi:10.4095/207617

Bristow, Q., 1979. Gamma ray spectrometric methods in uranium exploration – airborne instrumentation; *in* Geophysics and Geochemistry in the Search for Metallic Ores, (ed.) P.J. Hood; Geological Survey of Canada, Economic Geology Report 31, p. 135–146. doi:10.4095/106037

Bristow, Q., 1983. Airborne γ-ray spectrometry in uranium exploration, principles and current practice; The International Journal of Applied Radiation and Isotopes, v. 34, Issue 1, p. 199–229. doi:10.1016/0020-708X(83)90127-8

Conaway, J.G. and Killeen, P.G., 1978. Quantitative uranium determinations from gamma-ray logs by application of digital time series analysis; Geophysics, v. 43, no. 6, p. 1204–1221. doi:10.1190/1.1440888

Conaway, J.G. and Killeen, P.G., 1980. Gamma-ray spectral logging for uranium; Canadian Mining and Metallurgical Bulletin, v. 73, no. 813, p. 115–123.

Devoto, R.H., 1978. Uranium geology and exploration; lecture notes and references; Colorado School of Mines, Golden, Colorado, 396 p.

Dodd, P.H. and Eschliman, D.H., 1972. Borehole logging techniques for uranium exploration and evaluation; *in* Uranium Prospecting Handbook, (ed.) S.H.U. Bowie, M. Davis, and D. Ostle; Institute of Mining and Metallurgy, London, United Kingdom, p. 244–276.

George, D.C., 2007. Calibration of total-count gamma ray probes for estimation of uranium resources. <http://www.deltaepsilon.com/cal_paper.htm> [retrieved September 12, 2007]

Grasty, R.L., 1977. A general calibration procedure for airborne gamma-ray spectrometers; *in* Report of Activities, Part C; Geological Survey of Canada, Paper 77-1C, p. 61–62.

Györfi, I., Hajnal, Z., Bernier, S., Takacs, E., Reilkoff, B., White, D., Powell, B., and Koch, R., 2002. Initial seismic images along line 14 of the McArthur River high-resolution survey; *in* Summary of Investigations 2002; Saskatchewan Geological Survey, Saskatchewan Industry Resources, Miscellaneous Report 2002-4.2, Paper D-3, 5 p.

Hovdan, H. and Bolviken, B., 1985. Sulphide self potentials in relation to oxygen content in drill-hole water; Geoexploration, v. 23, p. 387–394. doi:10.1016/0016-7142(85)90004-3

International Atomic Energy Agency, 1986. Practical borehole logging procedures for mineral exploration, with emphasis on uranium; IAEA Technical Report 259, 44 p.

International Atomic Energy Agency, 2009. World distribution of uranium deposits (UDEPO), with Uranium Deposit Classification; IAEA TECDOC-1629, 115 p.

Jefferson, C.W., Thomas, D., Quirt, D., Mwenifumbo, C.J., and Brisbin, D., 2007. Empirical models for Canadian unconformity-associated uranium deposits; *in* Proceedings of Exploration 07: Fifth Decennial International Conference on Mineral Exploration, Toronto, Ontario, September 9–12, 2007, (ed.) B. Milkereit; Decennial Mineral Exploration Conferences, Toronto, Ontario, p. 741–769.

Killeen, P.G., 1979. Gamma ray spectrometric methods in uranium exploration—Applications and interpretation; *in* Geophysics and Geochemistry in the Search for Metallic Ores, (ed.) P.J. Hood; Geological Survey of Canada, Economic Geology, Report 31, p. 160–229. doi:10.4095/106037

Killeen, P.G., 1983. Borehole logging for uranium by measurement of natural gamma radiation — a review; The International Journal of Applied Radiation and Isotopes, v. 34, no. 1, p. 231–260. doi:10.1016/0020-708X(83)90128-X

Killeen, P.G., 1997. Mine site exploration and ore delineation nuclear techniques for ore grade estimation; *in* Proceedings of Exploration 97: Fourth Decennial International Conference on Mineral Exploration, Toronto, Ontario, September 14–18, 1997, (ed.) A.G. Gubins; Prospectors and Developers Association of Canada, Toronto, Ontario, p. 677–684.

Killeen, P.G. and Carmichael, C.M., 1970. Gamma-ray spectrometer calibration for field analysis of thorium, uranium and potassium; Canadian Journal of Earth Sciences, v. 7, no. 4, p. 1093–1098. doi:10.1139/e70-102

Killeen, P.G. and Elliott, B.E., 1990. Model boreholes for gamma-ray logging: intercalibration of North American and European calibration facilities; *in* Transactions of the 13th Society of Professional Well Log Analysis European Formation Evaluation Symposium, Budapest, Hungary, October 22–26, Paper GG, 14 p.

Killeen, P.G. and Mwenifumbo, C.J., 1988. Downhole assaying in Canadian mineral deposits with the spectral gamma-gamma method; *in* Current Trends in Nuclear Borehole Logging Techniques for Elemental Analysis; International Atomic Energy Agency, IAEA-ECDOC-464, p. 23–29.

Killeen, P.G., Bristow, Q., and Mwenifumbo, C.J., 1983. Gamma-ray logging for uranium: status of international efforts to resolve discrepancies in calibration models; *in* Transactions of the SPWLA (Society of Professional Well Log Analysts) 24th Annual Logging Symposium, Calgary, Alberta, June 27–30, 1983, Paper AA, p. 1–16.

Killeen, P.G., Bernius, G.R., and Mwenifumbo, C.J., 1995. Surveying the path of boreholes: a review of orientation methods and experiences; *in* Proceedings of the 6th International MGLS Symposium on Borehole Geophysics for Minerals, Geotechnical and Groundwater Applications; Santa Fe, New Mexico, October 22–25, p. 1–25.

McBride, D. and Workman, A., 2005. Review of the Agnew Lake Uranium Mine, Hyman Township; Ontario; technical report for Ursa Major Minerals Inc; Watts, Griffis and McOuat, Toronto, Ontario, <http://www.infomine.com/index/pr/Pa275170.PDF>[accessed April 22, 2008].

Mwenifumbo, C.J., 1990. Optimization of logging parameters in continuous time domain induced polarization measurements; *in* Proceedings of the 3rd International Symposium on Borehole Geophysics for Minerals, Geotechnical and Groundwater Applications, 2–5 October 1989, Las Vegas, Nevada, Paper N, p. 201–232.

Mwenifumbo, C.J., 1993. Temperature logging in mineral exploration; Journal of Applied Geophysics, v. 30, p. 297–313. doi:10.1016/0926-9851(93)90038-Z

Mwenifumbo, C.J., 1997. Electrical methods for ore body delineation; mine site exploration and ore delineation; *in* Proceedings of Exploration 97: Fourth Decennial International Conference on Mineral Exploration, Toronto, Ontario, September 14–18, 1997, (ed.) A.G. Gubins; Prospectors and Developers Association of Canada, Toronto, Ontario, Paper 85, p. 667–676.

Mwenifumbo, C.J. and Bernius, G., 2007. A Th rich crandallite group mineral: a source of thorium enrichment in the Athabasca Group, Saskatchewan; *in* EXTECH IV: Geology and Uranium EXploration TECHnology of the Proterozoic Athabasca Basin, Saskatchewan and Alberta, (ed.) C.W. Jefferson and G. Delaney; Geological Survey of Canada, Bulletin 588 (*also* Geological Association of Canada, Mineral Deposits Division, Special Publication 4; Saskatchewan Geological Society, Special Publication 18) p. 521–532. doi:10.4095/223742

Mwenifumbo, C.J., Elliott, B.E., Hyatt, W.G., and Bernius, G.R., 2005. Bells Corners calibration facilities for downhole and surface geophysical equipment; Geological Survey of Canada, Open File 4838, 17 p. doi:10.4095/216755

Paillet, F.L. and Cheng, C.H., 1991. Acoustic Waves in Boreholes; CRC Press, Boca Raton, Florida, 264 p.

Paillet, F.L., Cheng, C.H., and Pennington, W.D., 1992. Acoustic-waveform logging - advances in theory and application; The Log Analyst, v. 33, no. 3, p. 239–257.

Pflug, K.A., Killeen, P.G., and Mwenifumbo, C.J., 1994. Acoustic velocity logging at the McConnell nickel deposit, Sudbury area, Ontario: preliminary in situ measurements; *in* Current Research 1994-C, Geological Survey of Canada, p. 279–286.

Quirt, D. and Elash, T., 2006. Recalibration of the Saskatchewan Research Council uranium test pits; Saskatchewan Research Council Confidential Report, SRC Publication No. 10400–05C06, 17 p. (plus appendices).

Sato, M. and Mooney, H., 1960. The electrochemical mechanisms of sulphide self-potentials; Geophysics, v. 25, no. 1, p. 226–249. doi:10.1190/1.1438689

Stromswold, D.C. and Wilson, R.D., 1981. Calibration and data correction techniques for spectral gamma-ray logging; *in* Transactions of the SPWLA 22nd Annual Logging Symposium, Mexico City, Mexico, Society of Petrophysicists and Well Log Analysts, Paper M, p. 1–8.

Taylor, K.C., Hess, J.W., and Mazzela, A., 1989. Field evaluation of a slim-hole borehole induction tool; Ground Water Monitoring Review, v. 9, no. 1, p. 100–104. doi:10.1111/j.1745-6592.1989.tb01125.x

Wilson, H.C., Michel, F.A., Mwenifumbo, C.J., and Killeen, P.G., 1996. Application of borehole geophysics to groundwater energy resources; Journal of Environmental & Engineering Geophysics, v. 1, no. 1, p. 21–26.

World Nuclear Association, 2010. Geology of Uranium Deposits; <http://www.world-nuclear.org/info/inf26.html>[accessed January 5, 2012].

World Nuclear Association, 2011. World Uranium Mining; <http://www.world-nuclear.org/info/inf23.html>[accessed January 5, 2012]

Geological Survey of Canada Project EGM007